Cost Reducing Optimization Strategies of Electrical Trains

BY

SOUMYA PADMANABHA SARMA
B.Tech., College of Engineering Trivandum, 2013
M.S., Indian Institute of Technology Madras, 2017

THESIS

Submitted as partial fulfillment of the requirements
for the degree of Master of Science in Electrical and Computer Engineering
in the Graduate College of the
University of Illinois at Chicago, 2020

Chicago, Illinois

Defense Committee:

Sudip K. Mazumder, Chair and Advisor
Lina He
Eduardo Pilo de la Fuente, EPRail

ACKNOWLEDGMENTS

I'm indebted to many people for their continuing support leading to this thesis. First, I would like to express my sincere gratitude towards my advisor Prof. Sudip K. Mazumder for his constant motivation, guidance and suppport. Many thanks to Dr. Eduardo Pilo de la Fuente for sharing his knowledge and supporting my research. I would also like to thank him and Prof. Lina He for serving in my thesis committee and providing their valuable insights on my research. I am also very indebted to Prof. K. Shanti Swarup and Prof. Dinesh Gopinath, my previous advisors at IIT Madras and College of Engineering Trivandrum for their constant motivation, encouragement and guidance.

I would like to extend my heartfelt gratitude towards my colleagues at the Laboratory of Energy and Switching Electronics System (LESES). Many thanks to my friends Ankit, Debanjan, Moien, Nikhil, Anik, Keertana, Sandeep, Shantanu and Congbo for their technical, moral and emotional support and valuable guidance throughout my MS program.

I would like to thank my husband Sri Krishna, my pillar of support, who has been constantly supporting and encouraging me in all my endeavors. With great pleasure, I express my sincere gratitude to my beloved parents Padmanabha Sarma and Jayasree, my sister Swetha and my inlaws for their constant love and support. And above all, I thank the Almighty for His guidance, strength, protection and tremendous blessings bestowed throughout my life.

SPS

PREFACE

This dissertation is an original intellectual product of the author, S. Padmanabha Sarma. All of the work presented here was conducted in the Laboratory for Energy and Switching-Electronics Systems (LESES) at the University of Illinois at Chicago. The main project “CPS: Breakthrough: Collaborative Research: Transactive Control of Smart Railway Grid” is funded by the National Science Foundation (NSF) under award number 1644874.

Soumya Padmanabha Sarma
March 25, 2020

CONTRIBUTION OF AUTHORS

Major parts of the results and discussions in this thesis are taken from my accepted paper with written permission from the (see Appendix B). S. Padmanabha Sarma, S. K. Mazumder and E. Pilo conceived the main ideas and led the investigations. S. Padmanabha Sarma undertook the simulations and S. K. Mazumder and E. Pilo contributed to the write-up of the conference publication.

TABLE OF CONTENTS

TABLE OF CONTENTS (Continued)

LIST OF TABLES

LIST OF FIGURES

FIGURE **PAGE**

LIST OF FIGURES (Continued)

LIST OF ABBREVIATIONS

RT	Real-Time
DA	Day-Ahead
RSG	Railway Smart Grids
ESG	Electrical Smart Grids
RPS	Railway Power System
RSO	Railway System Operator
ISO	Independent System Operator
LMP	Locational Marginal Price
NEC	North-East Corridor
ISO-NE	New England Independent System Operator
SEPTA	Southeastern Pennsylvania Transportation Authority
MARC	Maryland Rail Commuter
ERCOT	Electric Reliability Council of Texas
DE	Differential Evolution
ACC	Area Control Centers

SUMMARY

In this thesis, strategies for minimizing the cost of energy utilized for the trip of an electric train have been studied. Trains are spatio-temporally varying loads. The spatio-temporally varying nature and the regenerative capacity of the trains provide an excellent opportunity for purchasing and selling the same magnitude of power at different times and locations, according to the price of electricity, which also has spatio-temporal variations. This variation is the basis for two new mechanisms for minimizing the cost of electricity utilization in high-speed electrical trains being pursued in this thesis. In the first approach, unlike the traditional approach of minimizing the energy, we aim to minimize the weighted-cost of electrical energy since the cost of the latter varies with the spatio-temporal location of the train. In the second approach, we outline a transaction mechanism between an electrical train and a real-time electrical load such that the cost of electricity utilization by both may be reduced. Conventional approach to transaction is typically based on bulk and unidirectional power flow while this new approach extends it to distributed and bi-directional power flow. We have analyzed both of these approaches by varying different factors and have provided directions for future research.

CHAPTER 1

INTRODUCTION

We start by providing the background and motivation that led to this research. We then provide the literature review that shows the existing work in relevant areas. We conclude this chapter by outlining the contributions and an overview of each chapter.

1.1 Motivation and Objectives

Diesel locomotives succeeded their IC engines counter-part around 1930s and have been in use even now in many parts of the world (Van Lessen, 1950). With diesel-electric locomotives, the power is transmitted from diesel engines to the wheels via eletric transmission. Significant research work has been done on these types of trains for analyzing techniques to reduce the fuel consumption, which is essentially minimizing the energy consumed by the trains. Pontryagin's maximum principle was applied to this minimization problem that resulted in the optimal 4-mode trajectory-acceleration, cruising, coasting and braking phases on the flat railway tracks(Ichikawa, 1968; Howlett, 1990; Lee et al., 1982). But with the development of electric power systems, the diesel locomotives started being replaced by electric engines in many parts of the world. The advantages of electric locomotives compared to diesel locomotives as enlisted by the authors of (Moyer, 2016) are as follows:

- As the current trend of electricity prices are falling, it is 50 % cheaper to run electric locomotives than diesel locomotives.

- The running and maintenance costs of electric locomotives are 30-35 % lesser than that for the diesel locomotives.
- Replacing all diesel powered locomotives by electric would reduce the carbon footprint and reduce air pollution including all harmful gases that get released, which is extremely important as these trains pass through highly populated areas.
- Switching to electricity powered engines would give a chance to use cleaner fuels like renewable energy that would lead to lesser greenhouse gas emissions.

But the transition from diesel to electric locomotives really changed these two aspects when considering the trajectory optimization problems.

- Regenerative braking could be employed in electric trains which can enable bidirectional power flow (from electric power grid to the trains and from the trains back to the grid) as compared to the unidirectional power flow in the case of diesel trains (diesel engines to wheels only).
- Because of regenerative braking, the coasting mode could be replaced by the braking phase for optimal energy consumption (Khmelnitsky, 2000).

In the case of diesel trains, energy minimization implies fuel consumption minimization which inturn implies fuel cost minimization as the train carries the fuel. But in the case of electric trains, this may not be the case always,i.e, minimization of energy may not equate to minimization of cost of energy utilized. The electric train operators may enter into contractual agreements with electricity suppliers to use electricity at a fixed price or a variable price-like the day-ahead LMPs. Through this thesis, we would like to explore the cost minimization strategies for electric railways. The different driving strategy optimization techniques for diesel and electric locomotives are compared in Figure 1.

Energy management in electric railway systems is a huge challenge, considering the number and

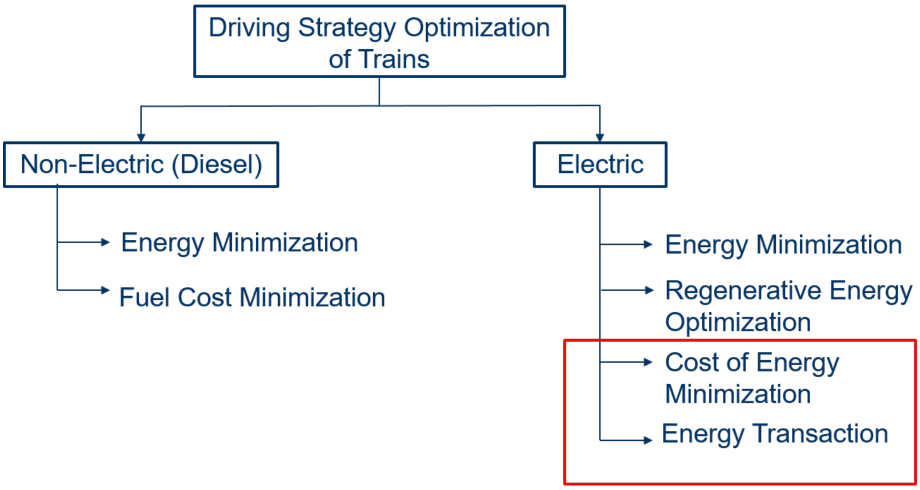

Figure 1: Driving strategy optimization of trains

type of players involved in it – trains, electric grid, way-side energy storage systems etc. The development of smart railway grids which involve pervasive sensing and coordinated information exchange between various participants in real time, yields distributed control and thus creates an exciting opportunity of integrating the scheduling of the train to the economy of its operation. The development of Electrical Smart Grids (ESGs) has been a major step towards addressing the environment quality and energy-consumption issues. The ESGs involve integrating information technology with electrical power systems which enhances their controllability. In a similar manner, the development of Railway Power

System (RPS) as Railway Electric Smart Grid (RESG) is particularly important because of the following reasons (De La Fuente et al., 2014):

1. The trains, which are spatio-temporally varying loads, are driven in different ways and hence can become even a generator during regenerative braking, making a change in power consumption from 10 MW to -8 MW in a few seconds.

2. The potential use of regenerative braking depends on when and where it is carried out.

3. The RPS span over large distances and may be interconnected to several grids. Efficient control is required to improve the economic operation of the system.

   A pictorial representation of power and traffic flow between the trains and various other components of an RESG is shown in the Figure 2 (De La Fuente et al., 2014).

One important aspect of the RESG is the possibility of the overall energy and operating-cost reduction with the smart interaction between the trains and the grid. The spatio-temporally varying nature and the regenerative capacity of the trains provide an excellent opportunity for purchasing and selling the same magnitude of power at different times and locations, according to the price of electricity, which also has spatio-temporal variations. This is not only effective for the high-speed long-distance trains, but also for the inter-city trains as well, as the frequency of travel is higher though the trip-distance is not longer.

The objectives of this thesis is identifying ways for minimizing cost of energy utlized by electric trains without compromising on their schedule by :

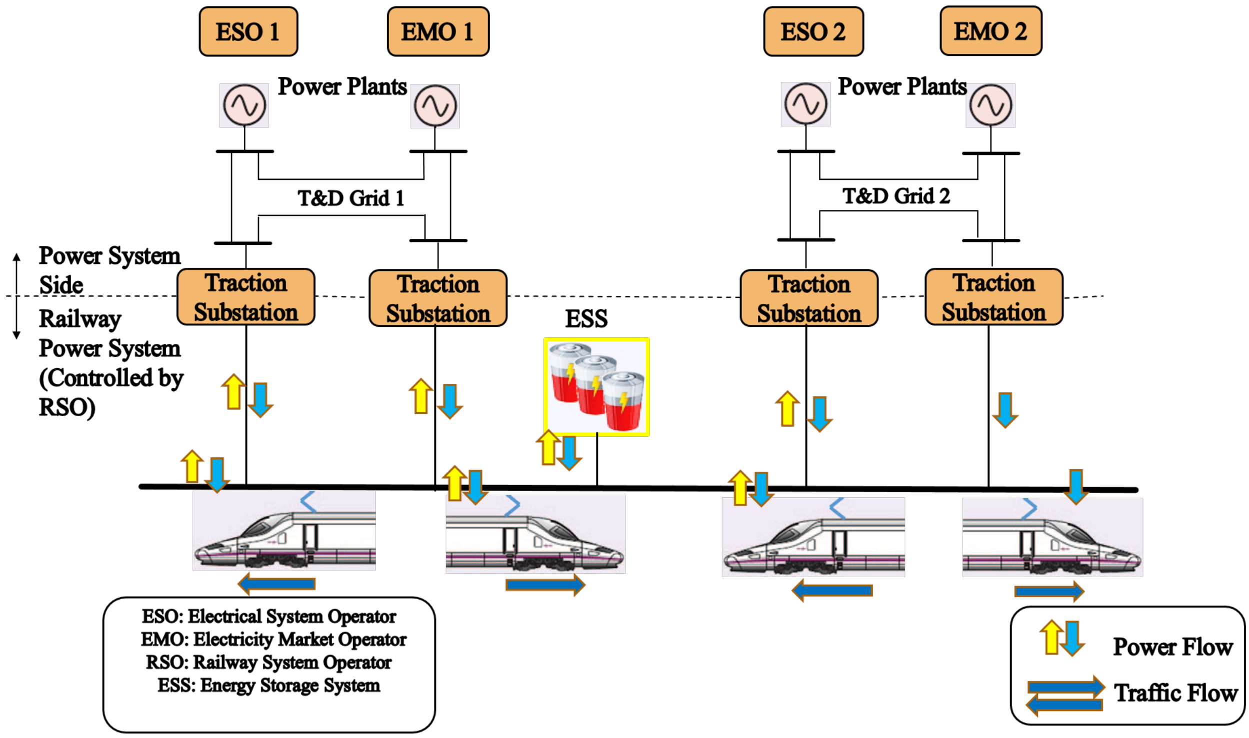

Figure 2: Bidirectional power flow between the different components of electric traction system

- Designing a weighted energy cost minimization objective framework utilizing the LMP prices or retail electriciy prices that varies with space and time.
- Utilizing energy transaction between trains and external loads that would reduce the cost of energy utilized for both the train and the load.

1.1.1 High Speed Electric Rail Network in the US

During the 20th century when most of the countries in the world invested in electric railway transportation, US companies chose to go ahead with diesel-electric technology because of less investment costs. The US railroads are private sector owned and would require huge funding for upgrading their systems to electricity-powered. Thus only less than 1% of the rail network inthe US is electrified. Amtrak's Acela express, North East Regional and Keystone services are the only high speed rail network in the US. The US High Speed Railway (USHSR) is an independent non profit organization that has detailed the plans for a 17000 mile national high speed railway system to be completed in different phases by 2030. The proposed route map is as shown in Figure 3(ush,) . The development of this HSR

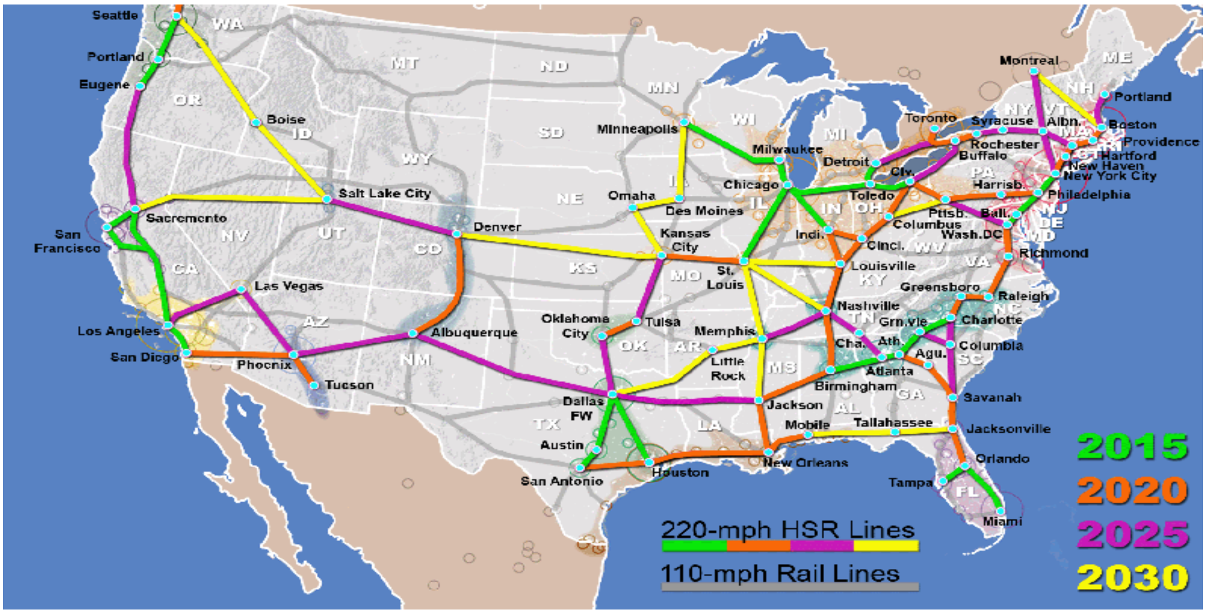

Figure 3: Proposed high speed rail network in the US

is projected to reduce congestion and carbon foot print along with improving the economy. Electricity costs occupy a major share of the running costs. We explore cost minimization strategies that would become beneficial for the developing high speed railway systems in the long run.

1.2 Literature Review

In this section, we review the existing methodologies for energy minimization of diesel and electric trains and transactive control as applied to other domains.

1.2.1 Optimal Control and Driving Strategies

Energy and environment quality concerns have made the energy optimal driving strategies for railway systems necessary. Currently, timetable and driving strategy optimization have been performed towards reducing the energy consumption. To meet the variable passenger demand, the railway operators schedule several timetables in advance and choose one based on passenger flow. Many formulations have been proposed for cyclic timetable formulation for minimizing passenger waiting times and delay times, headway-control, etc. (Nachtigall and Voget, 1997; Kroon and Peeters, 2003; Peeters, 2003). Many studies have analyzed efficient driving strategies for minimizing the energy consumption between stations. Driving strategy optimization is performed by considering different track conditions and optimal control strategies are found out for minimal energy consumption.(Cheng et al., 2000; Milroy, 1980; Howlett et al., 1994; Ichikawa, 1968; Howlett, 1990; Lee et al., 1982). The works (Ichikawa, 1968; Howlett, 1990; Lee et al., 1982) analyzed the Pontryagin's maximum principle for minimum energy consumption for various track conditions and trip durations and obtained the optimal operating modes of the trains. Regenerative braking has been employed for braking of the electric trains and is seen as a major contributor towards optimizing the energy consumption. In addition, the works of Benjamin, Cheng and Howlett (Benjamin et al., 1989; Jiaxin and Howlett, 1993; Howlett, 1996) optimized the speed profile for discrete values of traction force input, as the control mechanism of certain locomotives is not continuous.

Khmelnitsky (Khmelnitsky, 2000) considered the problem of energy minimization in a track with variable gradients and speed limit sections. He also showed that if regenerative energy can be fully recovered during the braking phase, the coasting phase will be interrupted in the optimal speed profile. The work of Li et. al demosnstrated that when considering the high speed trains, the 4-optimal modes do not hold true anymore and it will be only three optimal modes namely- acceleration, cruising and braking (Li et al., 2011). Studies have also been performed on adjusting the speed profile of the trains according to the braking time of other trains in a multi-train system to effectively utilize the recovered regenerative energy (Sun et al., 2014; Chen et al., 2015).

For the high speed train route of NorthEast Corridor (NEC) Acela express, we employ the 3 optimal modes for achieving the cruising speed of each speed limit section. The trajectory formulation based on speed limit sections are explained in Chapter2 Section 2.4 (Cheng et al., 2000).

1.2.2 Solution Methods

Different solution methods have been adopted to solve the optimization problem of minimizing the energy consumed.The authors of (Lin and Sheu, 2011), (Franke et al., 2000), (Howlett, 1990) have solved the driving optimization problem using the principles of optimal control. The authors of (Xu et al., 2014) employ dynamic programming to solve the optimal control problem. In (Miyatake and Ko, 2010), dynamic programming, Sequential Quadratic Programming (SQP) and gradient method have been compared for obtaining optimal velocity profiles where the authors state that SQP and gradient method can also control the state of charge of the energy storage devices. Artificial neural network and learning methods have also been employed for the energy and driving optimization of electric railways. (Pineda-Jaramillo et al., 2018; Martínez Fernández et al., 2019; Açıkbaş and Söylemez, 2008; Cai et al., 2017). They involve training the weights of the neural networks to achieve different objectives.

Another aspect has been the application of heuristics and evolutionary algorithms to solve the optimal switching strategy (Chang and Sim, 1997; Kim et al., 2013; Chevrier et al., 2011) (Jha et al., 2007; Domínguez et al., 2014; Sicre et al., 2014; Sheu and Lin, 2012). The algorithms - Clonal Selection (Dong et al., 2014), Model Predictive Control (Novak et al., 2018) Particle Swarm Optimization and its variants (Hu et al., 2014; He et al., 2019) Firefly-(Zhu et al., 2018; Keskin and Karamancioglu, 2016) Ant Colony GA-(Nasri et al., 2010),(Bocharnikov et al., 2010) MILP-(Lu et al., 2016) Comparing ACO, DP and GA- (Lu et al., 2013) comparing deterministic and heurictic algorithms-(Calderaro et al., 2015) have been used for obtaining optimal velocity profiles. They have an advantage over the numerical methods when it comes to solving complex systems, but their accuracy and speed are limited when it comes to solving real time systems. We have employed Differential Evolution (DE) to solve our optimization problems , where we had multiple speed limit sections whose holding speed was to be optimized using DE.

1.2.3 Cost Minimization and Transaction

Energy cost minimization is done in (Novak et al., 2017; Fleck et al., 2016), where the former talks about coordination of traction storages and trains energy consumption for cost efficiency and the latter explores the day-ahead optimization involving all components of the railway system. We apply the cost of energy minimization formulation to the electric trains utilizing the LMP prices along the route in the situation where the trains face the wholesale market price. When the trains face the retail supply charges, they are subjected to supply and demand charges which have also been taken into account. We also analyze the futuristic cases of longer and higher speed trains which are proposed to be introduced in the US for different % changes in electricity prices between the zones and compare the cost reduction percentages when employing cost minimization as opposed to energy minimization. Transactive control or market-based control is “a system of economic and control mechanisms that allow the dynamic balance of supply and demand across the entire electrical infrastructure using value as a key operational parameter” (Melton, 2015). Transactive control has been applied and tested on a few pilot projects in building management systems for control of responsive loads and have shown positive results (Melton, 2015; Somasundaram et al., 2014; Liu et al., 2018)(Katipamula et al., 2006). Standardisation of transaction is explained in (Hammerstrom et al., 2009), (Huang et al., 2010). PNNL has developed demonstration project on smart grid by involving residential customers from 12 utilities by building infrastructure with smart meters. (Sijie and Chen-Ching, 2017) covers the state of the art in transactive energy applications. In (Widergren et al., 2014), residential demand response is demonstrated by bidding transactions of air-conditioning appliances and supply. (Liu et al., 2017)(Hao et al., 2016; Behboodi et al., 2018) demonstate the transactive control applied to buildings and flexible residential loads. Transaction has also been applied to systems to obtain benefits other than cost reduction as in- (Yao and Zhang, 2017) for mitigating tie line fluctuations, (Subbarao et al., 2013) for providing ancillary services.

Transactive control has been extensively applied to residential loads and in few cases, electric vehicles, till date. We have not found the application of energy transaction to railway networks in existing literature. The concept of energy transaction and price negotiation explored in this thesis is slightly different as is explained in Chapter 4 and utilizes the flexible and regenerative braking concept of electric trains.

1.3 Thesis Organization

The remainder of the thesis is organized as follows. Chapter 2 establishes the electric train model and also details the concept of transaction, the trajectory formulation and the solution method for the optimization problem. It lays the basis for the cost minimization strategies adopted in this thesis. In Chapter 3, we demonstrate the reduction in cost of energy utilization obtained by optimizing the trajectory with time and space varying electricy price and compare the results with the cost obtained with energy-optimized velocity profiles. A portion of the NEC Acela Express train route has been used to test the cases. For providing insight on the future applications, we have demonstrated the results through parametric plots and compared different cases which also sheds light on the scheduling aspect. In Chapter 4, we explain the concept of energy transaction between electric train and an external load and also between electric trains. Different scenarios of this transaction have been explored for single and two train cases. Finally, we conclude our findings in Chapter 5 and also suggest possible directions for advancing the research on transactive control of railway smart grids.

CHAPTER 2

BACKGROUND AND MODEL

This chapter explains the fundamental concepts of modeling, trajectory formulation and optimization methods that are used to obtain the results in the successive chapters. Section 2.1 talks about the traction systems for electric railways, Section 2.2 describes the electric train model, Section 2.3 details the ways of utilizing the regenerative braking of the electric trains. Section 2.4 explains the method in which trajectory has been formed, 2.5 talks about the LMP generation by the ISOs, 2.6 explains the concepts behind applying the cost optimization techniques, and Section 2.7 explains the Differential Evolution optimization used for obtaining the optimal velocity profiles.

2.1 Electric Traction System

Electric traction system refers to the type of sypply system for the electricity powered locomotives. A wide range of frequencies and voltages (DC: 300, 500, 600, 750, 1200, 1500, and 3000 V, AC: 15 kV at 16.7 Hz, 25 kV at 60 Hz, 12 kV at 60 Hz, 11 kV at 25 Hz) have been in use across the different traction power stations across the world. A traction system architecture is depicted in the Figure 4 below. A traction system consists of overhead supply lines connecting different substations and the power is transferred to the trains through catenary-pantograph arrangement. There is an additional transformer-rectifier arrangement for AC traction systems feeding the DC motors.

Amtrak's Acela express interacts with 25 kV 60 Hz traction system during its northern end of the journey, from Boston, MA to New Haven, CT and with 11 kV 25 Hz traction system during its south-

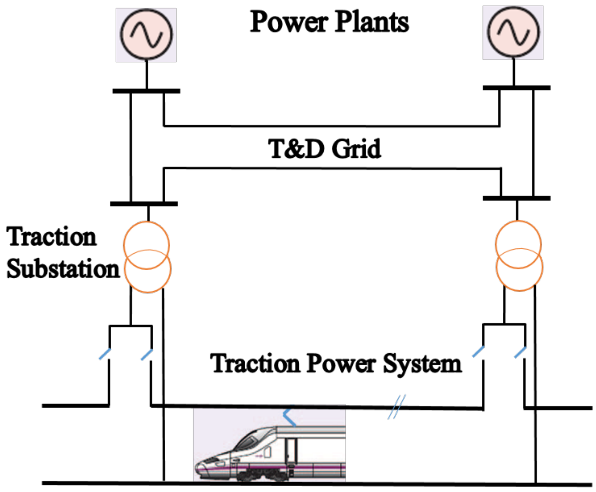

Figure 4: A traction power system architecture

ern end of the journey, from New York to Washington D.C. There are different substations, switching stations and paralleling stations along the electrification route. The LMPs at each of these substations are determined by the ISO and they are different owing to the different congestion levels and energy losses along the transmission system. Thus the electricity cost faced by the trains when crossing each of these pricing nodes are different. In the case where the train operators are locked to the wholesale LMP prices, the location of these nodes and their electricity prices during different hours of the day play an important role in determining the cost of energy utilization of each trip.

2.2 Electric Train Model

2.2.1 Assumptions

1. The mass of the train is assumed constant throughout the simulation and is multiplied by a factor of 1.1 to consider the rotational effect.

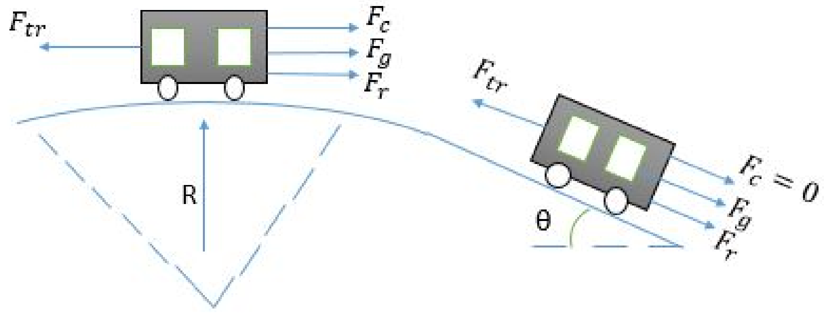

Figure 5: Forces acting on a train travelling through a slope and curve

2. The traction force and the braking force depend on velocity and they can be varied continuously.
3. With regenerative braking capabilities, the energy conversion efficiencies are assumed to be 70%.

2.2.2 Model

The forces acting on a train traveling through an elevation of angle θ and curve of radius R is depicted in Figure 5. The traction force is the input to the train for towing it forward. The various resistive forces acting on the train are the ones dure to air drag, rolling friction, gradient and curve reistances. A single train running on a track is goverened by the dynamical equation as shown below:

$$M * a = F_{tr}(v) - F_r(v) - F_c(s) - F_g(s) \tag{2.1}$$

s is the position of the train

M is the mass of the train (kg)

$F_{tr}(v)$ is the traction force of the train when travelling at a velocity v

$F_g(s)$ is the gradient resistance force at position s

$F_r(v)$ is the air drag and rolling resistance when travelling at a velocity v

$F_c(s)$ is the resistance due to curvature at position s

a is the acceleration of the train at position s

v is the velocity of the train

The traction force is obtained from the traction curve data. The formulae for F_r, F_g, and F_c are given below.

$$F_g(s) = M * g * \delta \tag{2.2}$$

$$F_r(v) = A + B.v + C.v^2 \tag{2.3}$$

$$F_c(s) = \begin{cases} M * g * D/1000/R(s), & R(s) > 10 \\ 0, & otherwise \end{cases} \tag{2.4}$$

where A, B, C, and D are empirical constants. The values are provided by our project collaborator Dr. Eduardo Pilo as $A = 3000$, $B = 143.64$, $C = 6.53184$, and $D = 302.54$. Symbol $R(s)$ is the radius of curvature at position s, δ represents the gradient of the track and g is the acceleration due to gravity. Tractive force is the force necessary to pull or push the locomotive to overcome the resistive forces like the gradient resistance force, air drag and rolling resistance, and curvature resistance. Locomotive

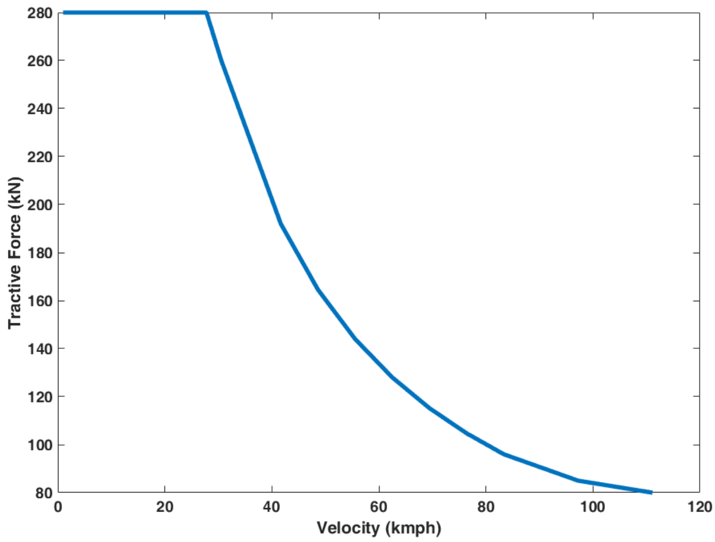

Figure 6: Tractive force curve as a function of velocity

manufacturers provide the tractive effort curve that is a function of input power and speed. The traction force as a function of speed used for simulations is shown in Figure 6.

Equation 2.4 shows the air drag and rolling resistance combined. This is the Davis equation which captures the rolling resistance with the first two terms A and Bv, and the drag resistance is captured by the Cv^2 term. The rolling resistance is predominant at lower speeds and the air drag at higher speeds.

The curvature resistance is experienced by the train when there are curves and bends and it is calulated based on the curvature radius. The gradient resistance is found based on the slopes and elevations in the track. Our project contributor Eduardo provided us the track data with curvature resistance, gradient, and speed limit sections of a Spanish high speed rail. We started our analysis with this track line and using all the track parameters we obtained the minimum time profile as shown in Figure 7. We have provided the data of this track in Appendix A. But for analyzing the profile with LMP information, we proceeded our analysis with the high speed Acela network in the US. Due to no published data on the track information of the route of the Acela express, we assumed a flat track for the Acela express.

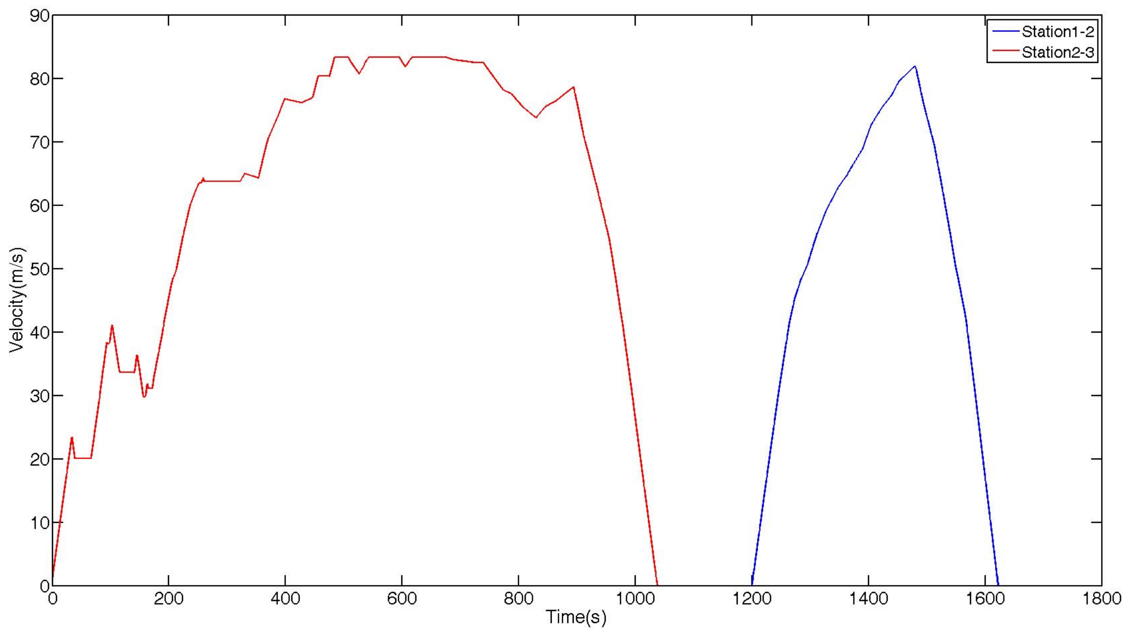

Figure 7: Tractive force curve as a function of velocity

The energy consumed to reach Station i in time T is given as:

$$E = \int_{t=0}^{T} P.dt \tag{2.5}$$

where P is the power consumed during the journey and is obtained as:

$$P = \frac{(F_{tr}(v) * v)}{\eta} + P_{aux} \tag{2.6}$$

During regenerative braking, the generated power P is gives as:

$$P = (F_{trb}(v) * v) * \eta + P_{aux} \tag{2.7}$$

where η is the efficiency of energy conversion. The utilization of regenerative energy may be limited by the power network and transmission loss, storage capacity at the substation, grid receptivity, etc. This is captured by the efficiency of conversion term η. Symbol $Ftrb$ is the braking force, P_{aux} is the power consumed by the auxiliary equipments like lighting and HVAC systems.

2.3 Regenerative Braking

Regenerative braking capabilities in an electric train is one of the key aspects in energy consumption minimization that distinguish it from its diesel counterpart.

The advantages and disadvantages of employing regenerative braking were discussed in the literature as early as 1932 (Gordon and Jaboolian, 1932). The various ways in which this regenerated energy can be utilized is depicted in Figure **??**. The energy generated can be utilized by an accelerating train in the same power zone. If there are no trains in the vicinity that can use up this energy, it can either be stored in the way-side energy storage systems or supplied back to the grid. SEPTA has installed batteries to capture this energy and claims to have a savings of 1380 MWh of energy savings after one year of its implementation, leading to almost half a million dollars (GabrielRéchard, 2017). If the traction power

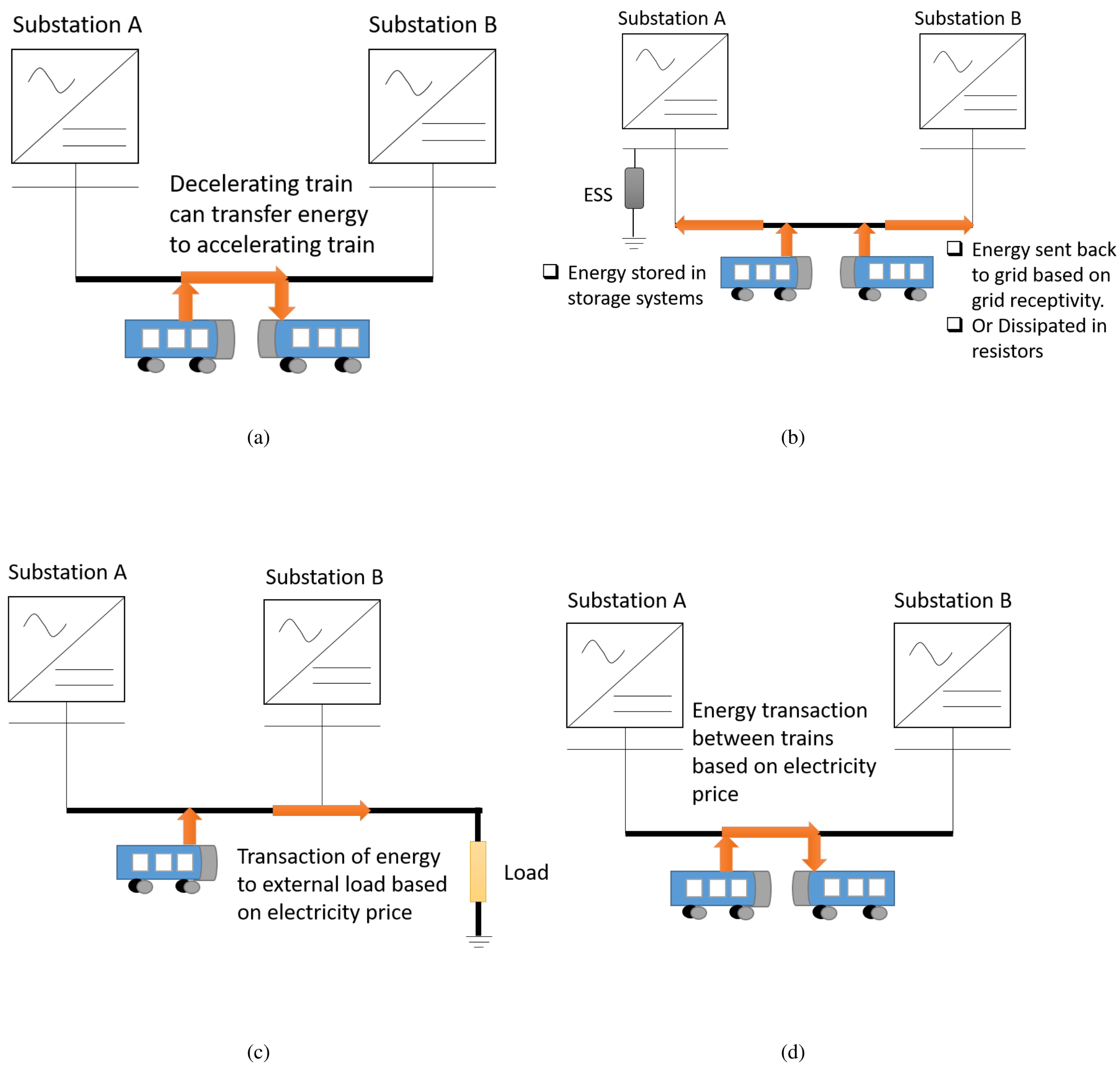

Figure 8: Different ways to utilize the energy generated by regenerative braking

system is bidirectional, then the utilization of the recovered energy depends on the grid receptivity. Due to limitations on grid receptivity, some of the energy generated may end up getting dissipated in the power resistors in the absence of energy storage devices. This captured energy can be used by the RSOs to participate in energy markets or frequency regulation markets leading to more profit for the railway system operators (GabrielRéchard, 2017). We have outlined the concept of transaction of energy between RSO and external load entities that utilizes this regenerated energy. The electric train network can cater to power request from external loads and enter into price negotiations that can be profitable for both the entities. Transaction can also happen between trains utilizing this regenerative braking energy depending on the electricity price vector.

2.4 Trajectory Formulation

The high-speed trains travel long distances which consist of a frequent change of slopes and curves, thus restricting the speed attainable at a particular section, leading to various speed limit sections. The optimization algorithm searches the speed value to be attained at every section. Once the speed value of the speed limit section is attained, it is followed until the end of the section unless the speed code of the next section is lesser than that of the current one. If the speed value of the next section is higher, the train accelerates to reach the higher speed value from the end of the current section. If the speed value of the next section is lower, the train decelerates from the braking distance at the current section to reach the lower speed value of the next section and the energy is recovered from regeneration. This makes the modes of operation as acceleration-cruising-and braking.

2.5 Locational Marginal Pricing

Locational Marginal Pricing denotes the value of electrical energy at different nodes of an interconnected system. Independent System Operators of a region determine the LMPs based on generation and demand bids by adhering to system constraints. The different ISOs operating in USA are shown in Figure 9 below. The ISOs determine electricity prices at their nodes that may be more than 1000

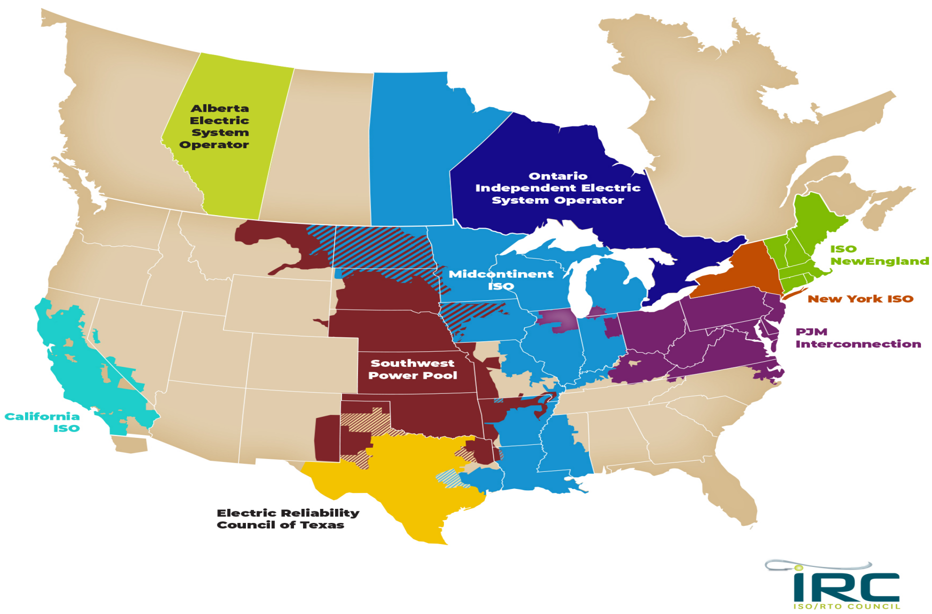

Figure 9: ISOs in operation in the North American region

and also at the system interconnections. The LMPs have three components as depicted in Figure 10 below: If the system has no transmission constraints or if there are no losses in the system, all LMPs ob-

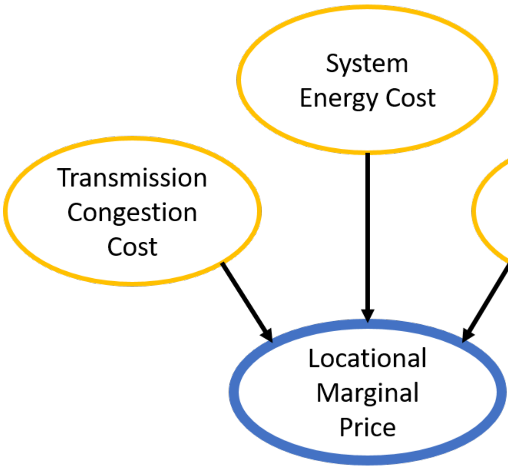

Figure 10: Components of LMP

tained through market clearing would be the same. Thus the loss component denotes the cost of system losses and the congestion component denotes the marginal cost of congestion at a given node relative to the energy component or load-weighted average of the system node prices (ig,).The ISOs calculate Day-Ahead (DA) and Real-Time (RT) LMPs based on the same basic calculation procedures, but there are certain differences between them. Theday-ahead nodal price is calculated based on minimum-cost, security-constrained unit commitment and dispatch that minimizes the costs of energy, transmission losses and congestion, with the system conditions, transmission outages already scheduled and existing line outages. Day-ahead energy market is analyzed to obtain the day-ahead nodal prices for each hour and real-time LMPs are calculated using real-time nodal prices every five minutes for the Real-Time energy market during the operating day. The real-time LMP optimizes both the electric energy dispatch and reserves.

2.6 Basis for Energy Cost Optimization

Energy minimization and cost of energy minimization would yield the same results in the case where there is no variation in the price of electricity. But in reality, there is a huge variation of electricity price with time and space as provided in the Figure 11 below which shows the hourly price variations of a particular day in a zone of ISO-NE and ERCOT.

For trains with longer trip distances like the Acela express which goes between MA and Washington D.C., it crosses different ISOs and hence different pricing zones. Hence the cost of energy is different at each zone owing to spatial variation of electricity price. The schedule of the trains will also have impact on the cost of energy owing to temporal variations in electricity price.

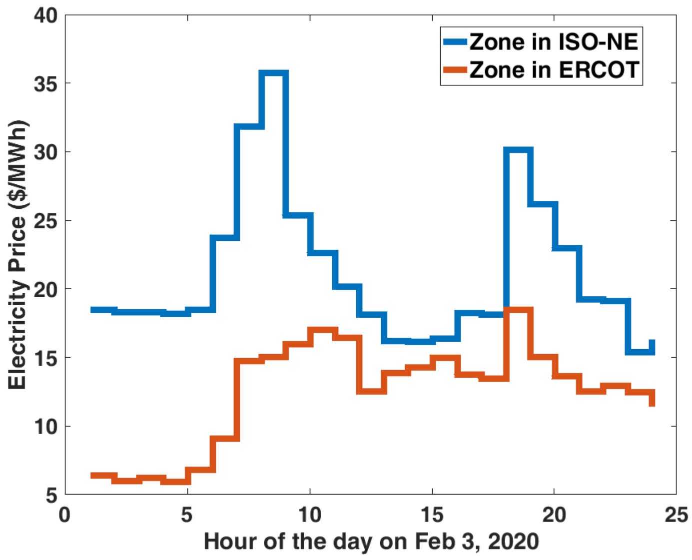

Figure 11: Hourly price variations of one of the pricing zones of ISO-NE and ERCOT on February 3, 2020

Trains are flexible demands and can have multiple velocity profiles for the same trip as shown in Figure 12(De La Fuente et al., 2014)(nsf,). This flexibility allows power consumption profiles to be adjusted to suit various needs like obtaining minimum energy profile, minimum time profile, minimum energy-cost profile, minimum power profile, etc.

This flexibility gives way to performing regenerative braking at specific times - for example, when the grid is stressed so that it can sell this energy, or to other trains that are in its vicinity. It is based on the concepts of spatial and temporal variation of electricity price and flexibility of power consumption of electric trains that we have performed our further analysis.

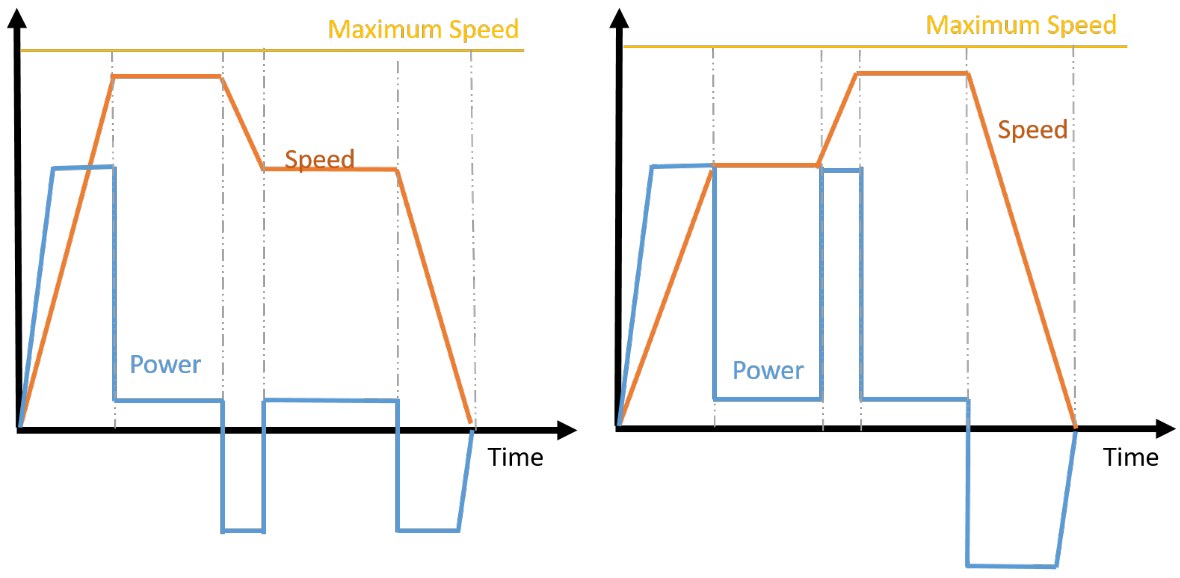

Figure 12: Two different velocity profiles with same trip distance and end time with different power profiles.

2.7 Optimization

The differential evolution (DE) algorithm has been used to search for an optimal speed value to be reached at every speed limit section. DE can be used for global optimization for functions that are non-convex, non-linear, multi-dimensional, or that have many local minima and constraints. When upgrading the simulation to a multi-train system, DE would prove beneficial as the problem search space gets increased.

Differential evolution is a stochastic population-based optimization algorithm developed by Storn and Price in 1996 (Storn and Price, 1997). DE is a parallel direct search method which considers N, D-dimensional parameter vectors $x_i, i = 1, 2 ... N$ as a population for each generation G. N remains constant during the process of minimization. The initial vector population is chosen randomly and should cover the entire parameter space. Uniform probability distribution is assumed for all random decisions. The flowchart for optimization with DE is given in Figure 13 and the generation of initial population vector is illustrated in Figure 14. DE generates new vectors of parameters by adding to the third vector, the weighted difference between two population vectors, called mutation process. This new mutated vector's parameters are combined with that of another predetermined vector, called the target vector, which outputs the trial vector. This step is called cross-over. The trial vector replaces the target vector in the next generation if its fitness evaluates to a lower cost value than the target vector. This process is called as selection. N competitions happen in one generation as each population vector will serve as target vector once. For our problem, the optimization variables are chosen to be the velocity values to be achieved at each speed limit section, in order to achieve certain objectives. The basic strategies of DE are explained below.

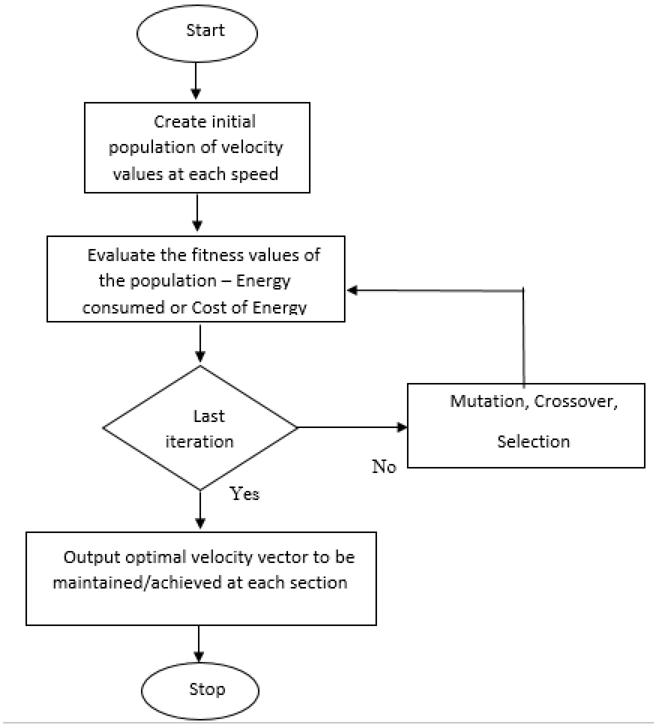

Figure 13: Flowchart for optimization with DE

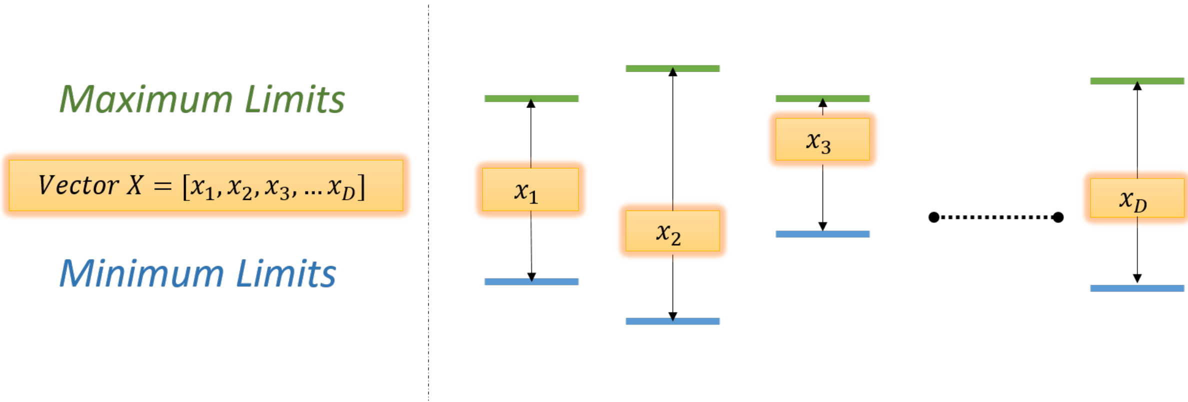

Figure 14: Illustration of initialization of population vector of size D

2.7.1 Mutation

For each target vector $x_{i,G}$, i=1,2..N, a mutant vector called as a donor vector is generated according to

$$v_{i,G+1} = x_{a,G} + F \times (x_{b,G} - x_{c,G}) \tag{2.8}$$

where $a, b, c \in$1,2..N are mutually different and also from index i, which necessitates $N \geq$4. F is a constant and real factor $\in$ [0,2] which contols the amplification of $(x_{b,G} - x_{c,G})$. This is illustrated in Figure 15.

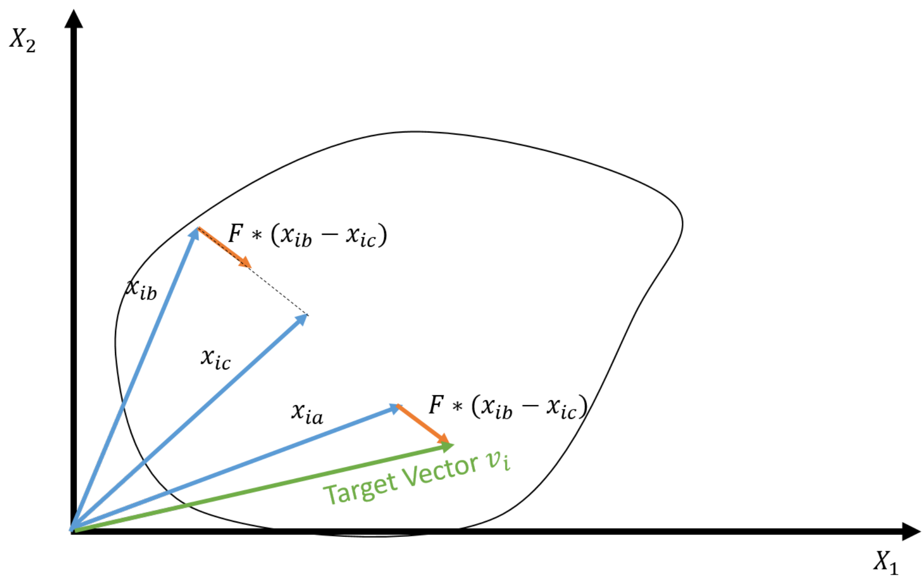

Figure 15: Illustration of mutation

2.7.2 Cross-over

The trial vector $u_{i,G+1}$ is developed from the elements of donor vector $v_{i,G+1}$ and target vector $x_{i,G+1}$ to enable diversity among the vector parameters, so that the elements of the donor vector enter into the trial vector with a probability of CR, a user determined cross over constant $\in [0,1]$. This process is illustrated in Figure 16.

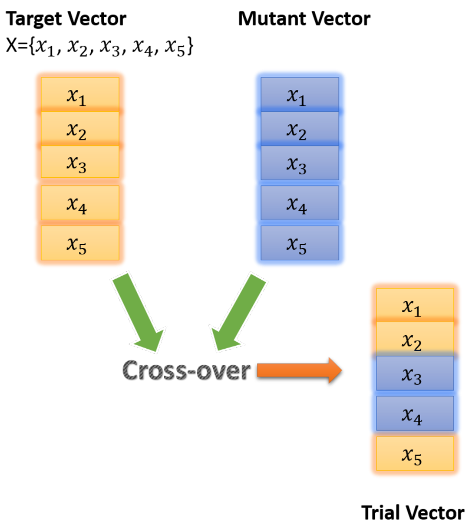

Figure 16: Illustration of cross-over

$$u_{j,i,G+1} = \begin{cases} v_{j,i,G+1}, \; if \; (rand(j) \leq CR) \; or \, j = I_{rnd}(i) \\ x_{j,i,G+1}, \; if \; (rand(j) > CR) \; and \, j \neq I_{rnd}(i), j = 1,2...D \end{cases} \tag{2.9}$$

where $rand(j)$ is the j^{th} evaluation of uniform random number generator with outcome $\in [0,1]$. $I_{rnd}(i)$ is a randomly chosen index $\in 1,2...d$ which makes sure that the trial vector gets atleast one parameter from donor vector.

2.7.3 Selection

The trial vector $u_{j,i,G+1}$ and target vector $x_{i,G}$ is compared and the one with the lower cost function is permitted to the next generation.

$$x_{i,G+1} = \begin{cases} u_{i,G+1},\ if\ f(u_{i,G+1}) \leq f(x_{i,G}) \\ x_{i,G},\ otherwise \end{cases} \tag{2.10}$$

The mutation, cross-over and selection continue until some stopping criterion is reached.

2.8 Summary

In this chapter, we looked into the electric train model and the ways in which regenerative energy can be utilized. We also discussed about the basis for the energy-cost optimization and also explained the strategies of the differential evolution optimization framework used in this thesis.

CHAPTER 3

MININUM COST OPERATION

Parts of this chapter is accepted for publication as(Soumya P. Sarma, 2019), IEEE

In this chapter, we formulate the cost minimization optimization of electric trains as described in Section 3.1. A comparison with energy minimization is done in order to see the benefits of cost optimization over energy optimization for various scenarios. A section of Amtrak's North-East Corridor profile has been selected for our analysis. This chapter is organized as follows. Section 3.1 describes the energy and cost optimization formulation, the objective and the constraints considered in our analysis. Section 3.2 explains the results obtained for various cases considered- when considering LMP pricing only and when considering utility demand charges.

3.1 Energy and Cost Optimization Formulation

As described in Chapter 2, electric supply feeds power to the traction motors and other auxilliary equipments like HVAC and lighting systems of an electric train. Optimizing the usage of electricity such that it minimizes the total electricity cost is vital for the train operators as millions of dollars are spent in electricity procurement. The optimization block diagram is presented in Figure 17. The solver which is the Differential Evolution optimizer takes the inputs as the train model, constraints and the schedule of the trip and optimizes the velocity profile against the DA pricing information obtained from the ISO. In the formulation presented here for energy and cost minimization, we use time as the independent variable and compute the kinematic variables $s(n,t), v(n,t)$ and $a(n,t)$ at each instant for the N trips of

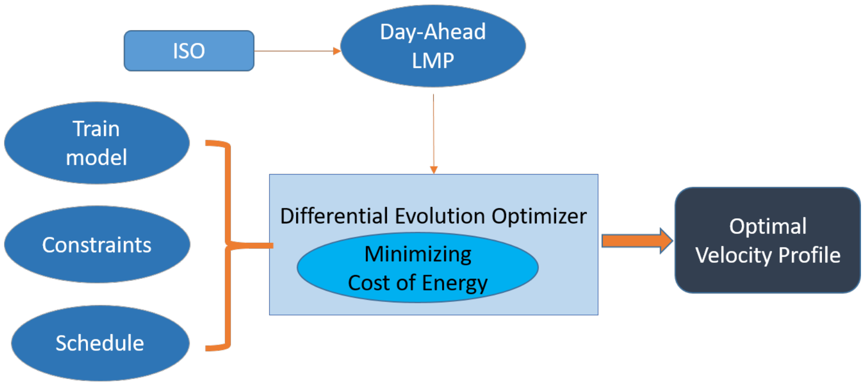

Figure 17: Optimization block diagram

a train that starts from position 0 and ends at position '$d(n)$' for each trip. The dynamics are presented in Section 2.2. We consider that the Area Control Centers (ACC) serve as the pricing zones. The electricity price $\lambda(i,t)$ denotes the electricity price (\$/MWh) in the region of ACC_i at time instant t and $P_i(n,t)$ denotes the power profile of the train at ACC i and trip n. As the train passes through different ACCs, its schedule determines the price for that trip. The objective function is shown in equations below. This can be extended to any number of schedules of the train, during which the prices at the ACCs vary over the day.

$$\text{minimize} \quad \sum_{n=1}^{N} \sum_{i=1}^{A(n)} \sum_{t=t_0(n)}^{T(n)} P_i(n,t)\lambda(i,t)$$

subject to

$$P_i(n,t) \leq P_i^{max}(n,t) \tag{3.1}$$

$$P_i(n,t) \geq P_i^{min}(n,t) \tag{3.2}$$

$$F_{tr}(n,t) \leq F_{tr}^{max}(v(n,t)) \tag{3.3}$$

$$F_{tr}(n,t) \geq F_{tr}^{min}(v(n,t)) \tag{3.4}$$

$$v(n,t) \leq v_{max}(s(n,t)) \tag{3.5}$$

$$v(n,t) \geq v_{min}(s(n,t)) \tag{3.6}$$

$$a(n,t) \leq a_{max}(s(n,t)) \tag{3.7}$$

$$a(n,t) \geq a_{min}(s(n,t)) \tag{3.8}$$

$$T(n) \leq T_{max}(n) \tag{3.9}$$

$$T(n) \geq T_{min}(n) \tag{3.10}$$

$$v(n,t_0(n)) = 0 \tag{3.11}$$

$$v(n,T(n)) = 0 \tag{3.12}$$

$$s(n,T(n)) = d(n) \tag{3.13}$$

$$s(n,t_0(n)) = d(n-1) \tag{3.14}$$

The constraints 3.1- 3.8 should be satisfied for all n and for all $t \in [t_0(1), T(N)]$. Constraints 3.9 through 3.14 are end point constraints on position $s(n,t)$, velocity $v(n,t)$ and trip time $T(n)$, which must be satisfied when the train reaches or leaves from the stations.

Constraints 3.5 through 3.8 imposes practical limitations on the values that can be achieved by the velocity and acceleration at any instant depending on its position. The trains pass through tracks with grades, curvatures, tunnels, stations etc, which determine its velocity limits along with the model of the train itself. For our simulation, the acceleration limits are considered to be $\pm 0.75 m/s^2$, which are usually decided keeping in mind the comfort level of the passengers. For very high speed trains, jerk constraints can also be included, which is the derivative of the acceleration.

The limits on the power consumption values as in consrains 3.1 and 3.2 are imposed by the ACC, the power being regenerated back to the grid is also limited by its storage capacity and receptivity. The constraints on the applied traction force as shown in 3.3 and 3.4 follow from the velocity limits.

3.2 Simulation Analysis

High speed rail network in the US is analyzed to choose the train route with higher speed and longer trip distance. Amtrak's Acela Express with maximum speeds of upto $250kmph$, Amtrak's Northeast Regional and Keystone Service, and MARC Penn Line express reaching maximum speeds of $201kmph$ are the only high-speed services in the country. Acela express route from Boston MA to New Haven, CT as shown in Figure 18 is considered for our simulation. The electric supply system for the NEC route of Amtrak is provided by the 60 Hz Traction power system between New Haven, CT and Boston, MA. There substations between Boston, MA and New Haven, CT are: Sharon, MA, Warwick, RI, New London, CT and Branford, CT, each containing two 115 kV/ 50 kV transformers. Norton, MA, Richmond, RI, and Westbrook, CT are the switching stations that transform 50 kV input to 25 kV voltage and separate the power zones. New England ISO, (ISO-NE) is the Independent System Operator for the NEC region of operation of Amtrak. All the price data, unless specified otherwise have been obtained from (ig,). For the trip of Acela that has been considered in our simulation, the trains pass through 4

Figure 18: Acela express route considered in the simulations

zones where the electricity prices vary with time. The pricing zones that are considered are NE Mass. (4008), SE Mass. (4006), Rhode Island (4005), and Connecticut (4004).

3.2.1 With LMP Pricing Only

In the situation where the RSO contracts for the wholesale energy pricing, the energy consumption is charged with the Locational Marginal Pricing (LMP). The cost minimization adjusts the power consumption of the trains according to the price vector along the track. When the price vector is the (LMP) along the track and the RSO contracts the electricity price for each hour Day-Ahead (DA), the RSO optmizes the profile of all the trains day-ahead according to the price at each substation along the journey of the trains.

The zonal day-ahead electricity pricing information has been obtained from (ig,) for June 27, 2019. The price difference between the zones of NE Mass. and SE Mass. are not significant. The hourly price variation between the zones are shown in Figure 19 and the results of energy and cost of energy optimization are compared in Table I. It can be observed that there is a huge price variation between the zones during the hours 15-20 and hence the trains that pass through these zones during these periods can make profit by performing cost of energy optimization. The price variation makes the optimizer choose the profile such that the energy consumed during the high-price hours is minimized. The results are compared in Figures 20.

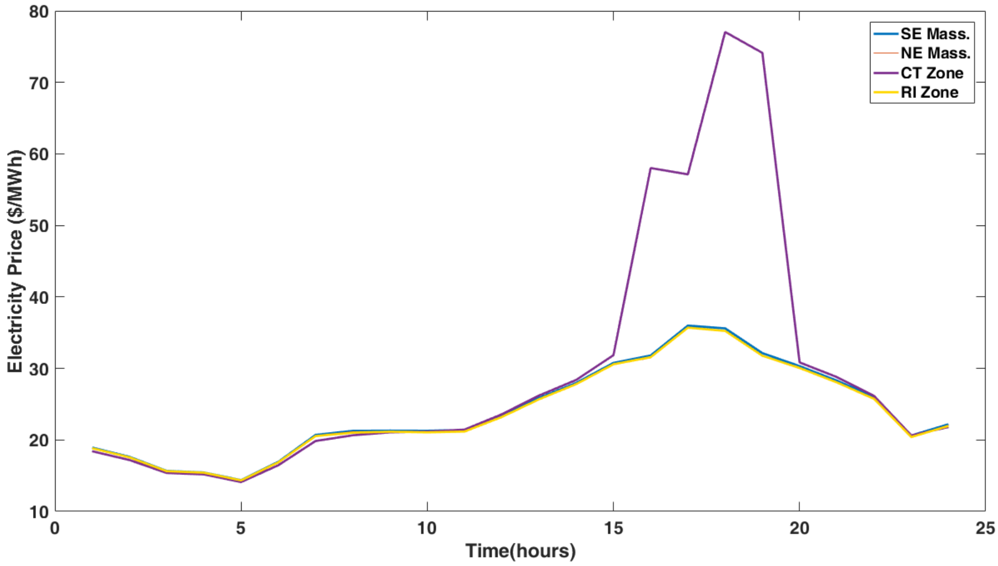

Figure 19: Price variation between the zones on June 27, 2019

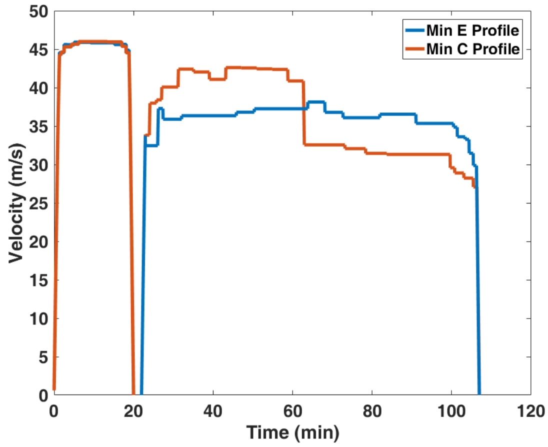

(a)

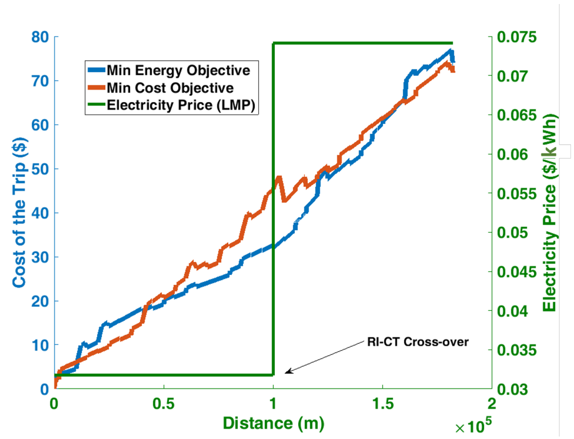

(b)

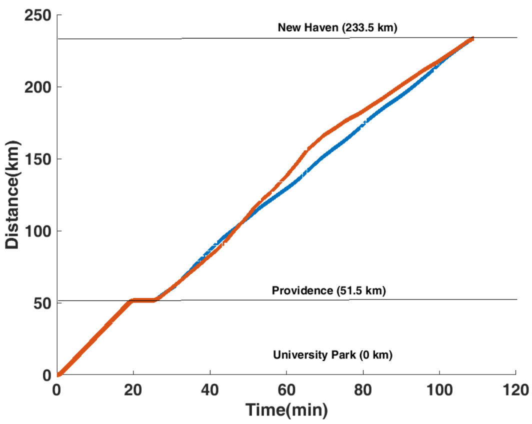

(c)

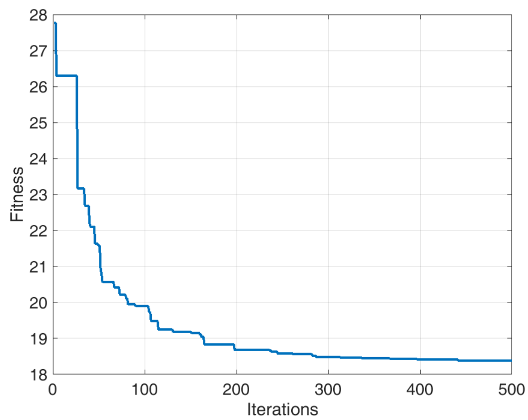

(d)

Figure 20: Comparison of cost minimization optimization with energy minimization optimization for University Park, MA to New Haven, CT route of the Acela Express. (a) Comparison of velocity profiles (b) Energy cost against time of journey (c) Distance profiles in the two cases. (d) Fitness value against iterations of DE optimization for University Park,MA to Providence, RI.

The schedule of the trains also determines the cost of energy utilization. As it is evident from the Figure 19, the electricity price variation between the two zones is not much during the hours before 3 pm and after 8 pm. Both of the optimization objectives would yield similar results when the price difference is not much. From the velocity profile, it can be verified that the trip time for the journey remains the same, whereas the brown curve achieves the minimum cost of energy operation. The Figure 7 (b) shows

	Minimization of Energy	Minimization of Cost of Energy
Cost of Energy ($)	91.2330	88.0215
Energy (MWh)	2.13	2.16

TABLE I: COST OF ENERGY UTILIZATION COMPARISON FOR ONE TRIP FROM UNIVERSITY PARK, MA TO NEW HAVEN, CT.

the cost of the trip against the trip duration. It can be observed that the minimum cost profile consumes more energy during lower price periods i.e., before the RI-CT crossover so that it finishes the trip with lower cost of energy utilization than the minimization of energy case. There is a reduction in cost of energy utilization by 3.5% for an increase in energy utilization of only 1.6%.

In order to assess the profit of cost optimization for a single day, cost of energy utilization for the trip between Providence, RI to New Haven, CT, for a weekday is found out.

The price difference between the contiguous zones could be anywhere between -0.01 \$/MWh and 112 \$/MWh based on our analysis. The hourly electricity price for February 4, 2016 is considered in our simulation which exhibits greater price variations as shown in Figure 21 and the results are compared in Table II. From the results, the weighted cost minimization has a profit of 14.53% over the energy minimization for all the trips from Providence, RI to New Haven, CT, for a single day. This comparison is valid only for the particular trip for a particular electricity price-day since the electricity prices vary widely over time and space.

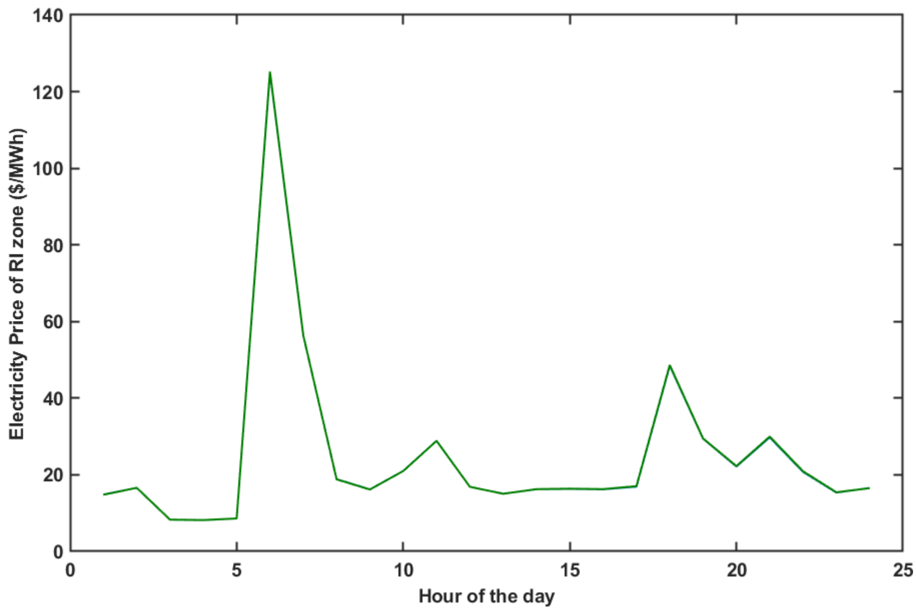

Figure 21: Price variation of the RI zone on Feb 4 2016

	Minimization of Energy	Minimization of Cost of Energy
Cost of Energy ($)	409.4751	349.4903

TABLE II: COST OF ENERGY UTILIZATION COMPARISON FOR ALL THE TRIPS FROM PROVIDENCE, RI TO NEW HAVEN, CT ON A SINGLE DAY.

This implies that the schedule of the train, its trip time, and the pricing zones through which it passes also affect the variation in cost of energy. To address the possible variations and to see the profitability with cost of energy minimization, the factors of zonal price variations, trip-distance, trip-time and % of regenerative energy available are varied and plotted as shown in Figure 22.

Figure 22 shows the% reduction in cost when employing cost minimization over energy minimization when the price difference between the zones considered vary by a factor of 1.3, 1.7 and 2. There are two pricing zones for this trip. The base case for all the figures have been energy minimization and the values obtained with cost minimization have been compared against them for the four different cases in Figure 22. Considering the Providence- New Haven trip of Acela express (182 km, 5100s trip) as the base case, we develop other cases by changing trip distance and time to obtain the comparison results. Figure 22a compares the cases for different trip distances of 90 km, 130 km and 180 km. The results show increasing benefits of cost reduction with longer trips and higher factor of price variations. The results are also indicative of a fact that longer the stops are, greater will be the benefits when employing the cost minimization.

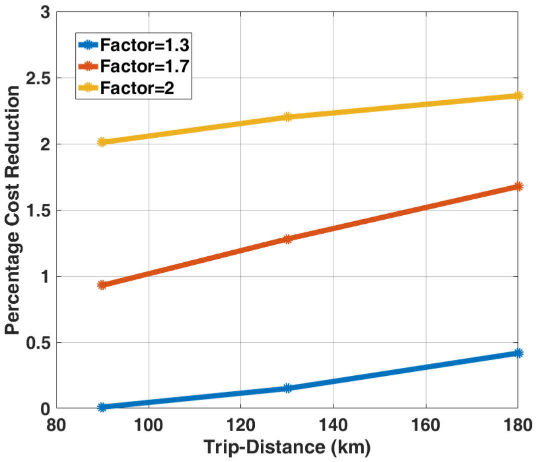

(a)

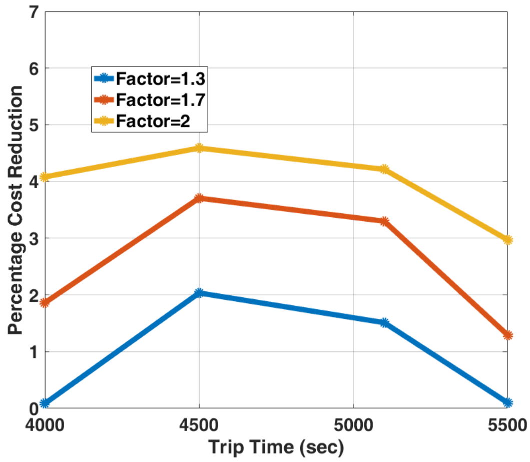

(b)

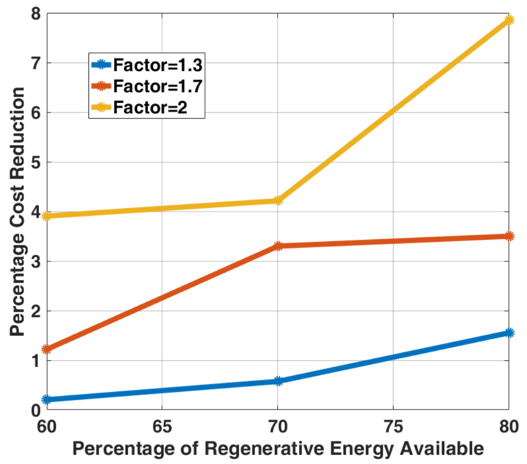

(c)

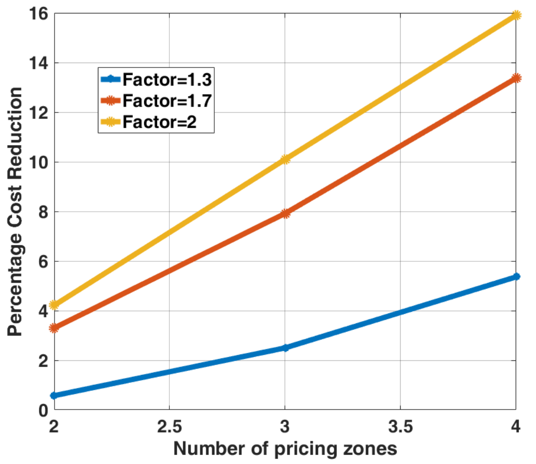

(d)

Figure 22: Parametric plots showing the reduction in energy cost with cost of energy optimization when compared to energy optimization. (a) Effect of trip distance (b) Effect of end times of the trip, and hence the maximum speed approaching the speed limits. (c) Effect of percentage of regenerative energy available after considering the efficiency factors (d) Effect of number of zones with price variations

Figure 22b shows the case of end time variation and thus the case when the speed gets closer to the maximum speed limits. For the trip of 182 km, trip times of 4000 s, 4500 s, 5100 s and 5500 s have been compared. The results indicate that that is an optimal trip time which shows maximum benefits when employing cost minimization. For very small and very large end-times, the benefits are not pronounced. With smaller trip times, the flexibility in adjusting the power consumption is not much and hence this factor cannot contribute to greater cost reduction. For longer trip times, both the minimization of energy and minimization of cost yield similar results so that the benefits are not pronounced. Figure 22c compares the % of regenerative energy available. Regenerative energy available for use is limited largely by the power transmission network, storage capacity at the substation, presence of other accelerating trains in the vicinity, grid receptivity among other factors. This is taken into account by the efficiency factor and comapred for 60, 70 and 80 percentages. The results show that the benefits are more pronounced with increasing regenerative energy percentages and with increasing factor of price difference between the zones.

Figure 22d compares the results when there are 2, 3, and 4 pricing zones. Since there can be large number of combinations of price factor variations between the consequtive zones, we have considered the case where all the consequtive zones are more than their previous zone values by a factor of 1.3, 1.7, and 2. From the patterns we can understand that there is a general trend of increasing benefits with more pricing zones and greater price variations where the consequtive zones have increasing electriciy prices.

These cases show the profitability of the approach when considering millions of dollars spent in electricity consumption for the whole year. From this it is clear that the benefits with cost minimization will be more pronounced when considering:

- Longer trips with higher speeds.
- Greater price variations between the adjacent zones.
- Schedule of the trips especially the trips during peak period.
- Greater availability of regenerative energy

The results are indicative of a proof that aiming for cost of energy utilization will lead to lesser cost of energy utilization when employed for all the trips of its journey. This shows that the cost of energy minimization will prove more profitable in the long run, when the US is expected to have a larger network of higher speed trains.

3.2.2 With Utility Demand Charges

When the RSO faces retail charges for its energy consumption, the utilities charge supply and delivery costs along with the demand charges. Demand costs are monthly charges that are evaluated by the maximum power consumed by the RSO during a month multiplied by the demand charges imposed by the utility.

	Minimization of Energy	Minimization of Cost of Energy
Yearly Cost for Providence-New Haven Trip ($)	1008000	924000

TABLE III: YEARLY COST OF ENERGY UTILIZATION COMPARISON FOR A SINGLE TRIP FROM PROVIDENCE, RI, TO NEW HAVEN, CT.

Generally, the demand charges are around 7$/kW (dem,). We compute the benefits of employing cost minimization over energy minimization for this case by assuming an average monthy cost of 60$/MWh and evaluating the cost of energy for an average of 20 % change in the price between the two zones. The railway operators spend millions of dollars towards energy costs. As shown above, even when considering the trip of Providence to New Haven for the whole year, the resulting cost savings are around 8.3%. When considering all the trips , the year-round savings with the cost minimization strategy is expected to be in millions of dollars.

3.3 Summary

In this chapter we discussed the benefits of employing cost minimization to obtain optimal velocity profiles and compared the results with energy minimized velocity profile and also showed the cases where the benefits are more pronounced. Although our results were based on analyzing a single trip, we have analyzed the results based on few assumed cases and summarized them in the parametric plots. The millions of dollars spent in the electric energy procurement by the railway companies can be efficiently reduced by employing the cost minimization optimization strategies as shown by our results.

CHAPTER 4

ENERGY TRANSACTION

Parts of this chapter is accepted for publication as(Soumya P. Sarma, 2019), IEEE Electric trains, using their flexibility in power consumption, can alter their velocity profile and transact energy with an external load. We have explored the conditions and cost reduction percentages in various cases of this transaction. This chapter discusses some possible scenario-centric transaction control opportunities.

4.1 Transaction Methodologies

Energy transaction can happen between trains and external loads in their vicinity and also between the trains as detailed below:

- When there is an external load controlled by the Load Serving Entity (LSE) that has an emergency power demand that is to be met, RPS can act as a transactive agent, willing to alter its power consumption during a stipulated time interval so that this relinquished energy can be utilized by the external load. The train can run an optimization check and determine whether it will be able to meet the schedule economically while still making profit.
- When there is an unexpected delay during a train's trip and it has to meet the schedule, it will require increased energy than the contracted amount. Transaction opportunities exist here as well where another train drawing power from the same substation can alter its consumption so that RPS, on the whole, can meet its schedule at equal or lesser energy costs, despite having to violate its contracted energy.

The energy transaction paves way for a dynamic adjustment in the electricity price at which the train is subjected to. This is shown in the block diagram of Figure 23.

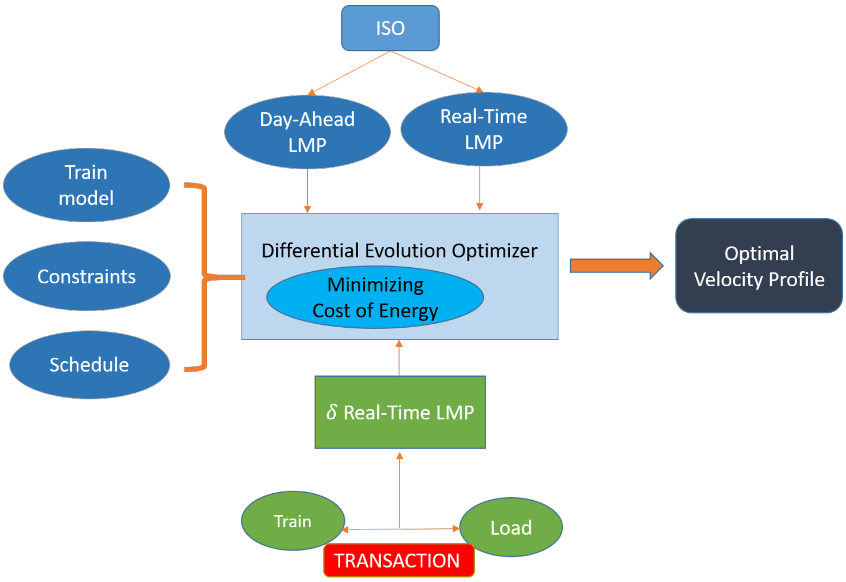

Figure 23: Transaction of energy with external load leading to dynamically changing the RT price to which the train is subjected to.

In the scenario where the real-time (RT) electricity price is higher than the day-ahead (DA) price, consider an external load L which has a sudden requirement of power for a small duration. The load L requests power from the adjacent transactive nodes where the RSG is one of them. Then the sequence of events follows as far as the train/ RSO is concerned.

1. The train runs a schedule check to determine if it can meet up with its original schedule within the allowed delay time by performing this transaction.
2. If yes for (1), then it runs an economic viability check to determine whether it will still be able to make profit if it adjusts its energy consumption in real-time.
3. If yes for (2), then the external load L and the train (RSO) negotiate the price that is to be paid by the load L to the train so that both the parties win.

When the train contracted the energy required for its trip day ahead, the ACCs lock the DA price with the ISO for the energy contracted. Any deviation in energy consumption from any of the ACCs would lead to the RSO paying the RT price for the excess energy consumed. The RSO may also be subjected to paying a penalty price for violating the contract. In our simulation, we have considered the penalty as paying the RT price for excess energy consumed.

When the external load requests the RSO, the information is sent to the respective ACCs which are in the vicinity of the load. The ACCs then run an optimization and profitability check and instruction is sent to the trains to alter their consumption accordingly. The objective for the ACCs is to bring down the cost of the trip and reduce the extra cost incurred due to energy transaction.

4.2 Transaction of Energy between Single Train and External Load

We have identified two ways in which transaction can be enabled between the train and the load. One is by reducing its energy consumption by the requested amount so that the load can use up this relinquished energy, called as cost-weighted demand shifting. The other is when there is enough storage capacities available at the substation/ station that the trains can generate energy by regenerative braking which can be stored by the storage units and consumed by the load according to its power profile.

4.2.1 Cost-Weighted Demand Shifting

We outline a transaction mechanism between the electrical train and an external load that would lead to reducing the cost of energy utilized for both the load and the train. From the conventional approach of bulk and unidirectional power flow based transaction, this new methodology extends it to a distributed and bidirectional power flow. This concept is based on the aggregate load demand for the ISO. The load aggregators aggregate the demands from various loads and this total demand is used for bidding at the ISO level. Consider an emergency load that requires power which it had not contracted day-ahead. We use the concept of demand shifting from train to the emergency load during high RT price periods using the the train's flexibility of power consumption. The total demand as seen by the aggregate load remains the same, but the trains can enter into negotiation with the external load for transacting the energy it requires.

Consider an emergency load which has not contracted its energy requirements with the ISO. This load will have to pay the RT price for the energy consumed. When the external load requires a certain amount of energy for a certain amount of time, the RSO can enter into negotiation with the load for decreasing the trains' energy consumption by the required amount so that this can be used by the load. We have performed the simulations for the case when the RT price is higher than the DA price in one zone and the RT price is equal to or lesser than the DA price in the subsequent zone. So, when the train reduces its velocity to reduce its energy consumption in the first zone, it can make up for the lost speed in zone 2 where the RT prices are lower than the DA prices. For example, the RT prices of February 3 and 4, 2016 have RT prices both higher and lower than the DA prices. We have analyzed the trip of Providence, RI to New Haven, CT with the following DA and RT prices as shown in Table IV.

Zone	DA Price ($/MWh)	RT Price ($/MWh)
1	50	100
2	55	55

TABLE IV: DAY-AHEAD AND REAL-TIME PRICES USED IN THE SIMULATION OF TRANSACTION BETWEEN TRAIN AND AN EXTERNAL LOAD

The formulation of this transaction is shown below.

$$\text{minimize} \quad \sum_{i=1}^{n} \lambda_i^{RT} \times (E'_{ACC_i} - E_{ACC_i}) + \lambda_i^{DA} \times E_{ACC_i}$$

subject to

$$E_{ACC_i}^{orig} - E_{ACC_i}^{act} = E_{load}^{req}, t \in [T_{req}] \tag{4.1}$$

In addition to 4.1, the constraints 3.1 - 3.14 also have to be satisfied. Symbol n denoted the total number of ACCs or pricing zones in the trip. Though this formulation is shown for a singletrip, this can be extended to any number of trips until the desired energy requested is achieved. The symbol E'_{ACC_i} denotes the excess energy consumed when participating in the transaction under pricing zone i, E_{ACC_i} denotes the contracted day-ahead energy consumption of ACC i with the ISO, λ_i^{RT} and λ_i^{DA} denote the electricity real-time and day-ahead price faced by the ACC i. The constraint 4.1 captures the energy transaction which means the requested energy has to be relinquished by the train for the duration requested. Symbol $E_{ACC_i}^{orig}$ is the original contracted energy consumption of ACC i during the requested time T_{req}, $E_{ACC_i}^{act}$ is the actual energy consumed during transaction and E_{load}^{req} is the actual energy requested by the load during T_{req}.

In the plots shown below in Figures 24a and 24b correspond to the case when the energy requested by the load is 300 kWh for 30 mins, that is, the train is transacting 20.16 % of its total energy consumed for a duration of 30% of its trip time.

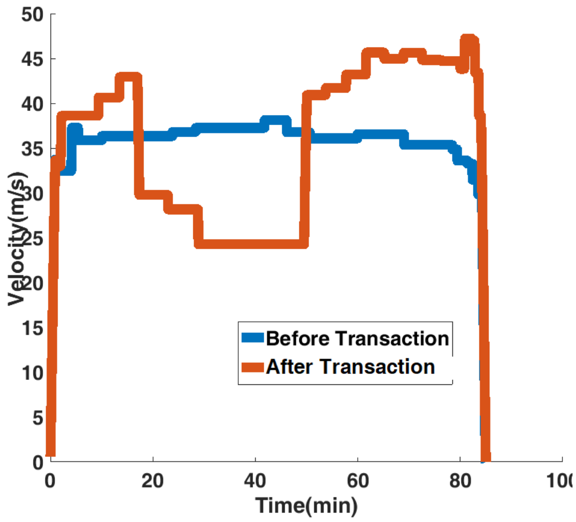

(a)

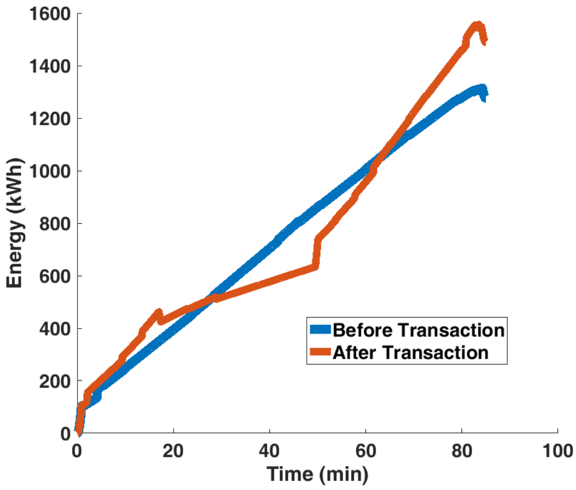

(b)

Figure 24: Energy transaction between train and external load. (a) Velocity profile of the train before and after transaction. (b) Cumulative energy profile before and after transaction

The train lowers its velocity for that duration so that this relinquished energy can be utilized by the load. In this case, the train is informed before starting its trip so that it can alter its profile accordingly. Figure 24a shows the velocity profile and Figure 24b shows the cumulative energy profile. Both indicate the adjusted profile by the train after transaction. The train can achieve a profit of 0-100% based on negotiation. When the RSO charges the load with the same price as the RT price, it receives a 28.47 % reduction in its cost of energy utilized and this value indicates the maximum reduction in cost obtainable for the train. But this will be a win for both parties if the load is charged less than the RT price and the train also receives profit even after incurring an excess cost for violating the contract with the ISO. Thus the profit and cost reduction percentages are dependent on the negotiation.

For the parametric plots below, we take the Providence to New Haven trip of 182 km, 5100 s trip and vary certain factors to obtain different plots. In Figure 25a, we vary the trip trime from 3600-5700s, the actual trip time being 5100s and perform energy transaction of 150 kWh for 20 mins and plot the maximum cost reduction percentage obtainable. With a very small trip time, after energy transaction, the train has to accelerate faster and reach the maximum speed again so that it doesn't violate the schedule constraints. When the trip time is larger, the actual energy consumed during the requested time of 20 mins is lesser, so that it has to brake more and travel at slower speeds inorder to transact the requested 150 kWh of energy. This could be the reason for lower cost reduction percentages with increasing trip time. But this trend is only true for this particular energy transacted amount and duration. The profit depends on all of these factors- that is, the trip time, trip distance, energy requested, duration of transaction, difference between RT and DA prices, negotiation, etc.

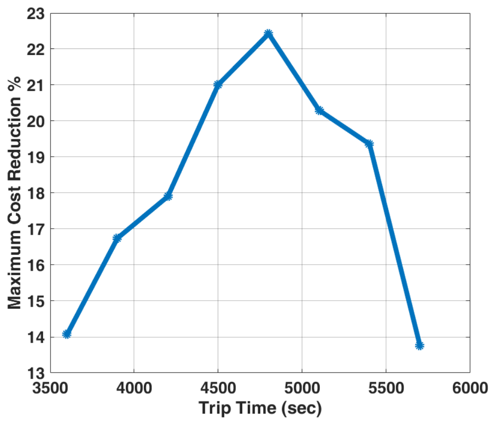

(a)

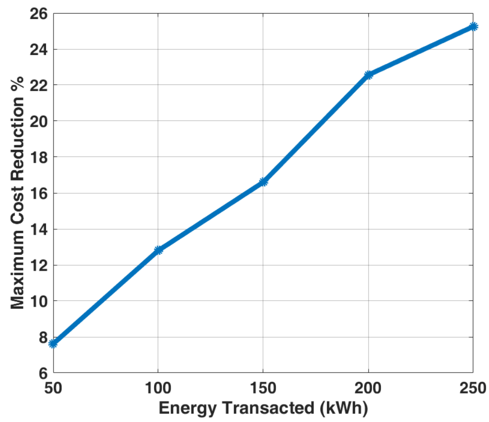

(b)

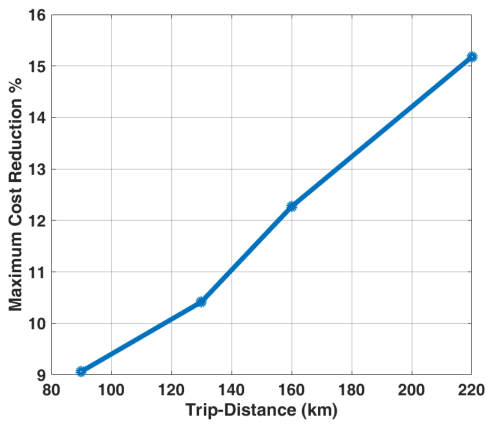

(c)

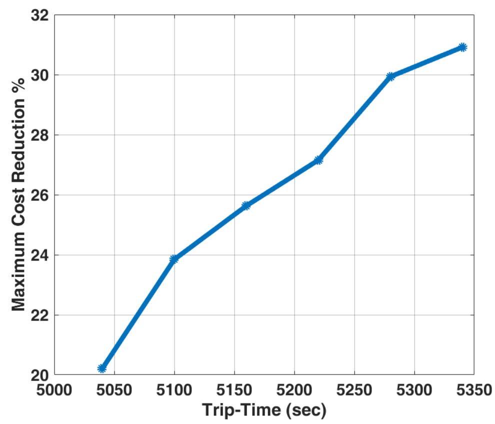

(d)

Figure 25: Parametric plots for the transaction of energy between train and external load. (a) Variation of maximum cost reduction percentage with trip-time. (b) Variation of maximum cost reduction percentage with energy transacted during 25-min duration (c) Variation of maximum cost reduction percentage with trip-distance. (d) Variation of maximum cost reduction percentage with allowed delay time

The Figure 25b below shows the maximum cost reduction percentages against the amount of energy relinquished in the 25 minute duration. With more energy transacted, the cost payable by the load increases more as compared to the excess cost incurred for the train due to this transaction. This is the reason for the increasing trend in maximum cost reduction percentages with increased energy transacted.

The Figure 25c shows the increase in cost reduction percentage with trip distance. For 90, 130, 160 and 220 km trips, the plot shows the cost reduction percentages of transaction for 20% of the total trip time duration and energy requested as 50 % of actual contracted values during that duration. This is for a 2-pricing zone case. Longer trips are more profitable as the trains can make up for the lost energy in the low price zone and the duration of travel in the low price zone is more. Certain delay times are allowed for a train in case it meets with some unexpected circumstances. We analyzed the profit for the train for every minute of delay time and observed the increase in cost reduction percentage as shown in Figure 25d.

4.2.2 Transaction with Available Storage Capacities

The trains release large amount of regenerative power in short time which can be stored in supercapacitors and released to meet the power requirements of the load. The available braking force determines the amount of energy released. The assumption here is the infrastructure which enables this kind of a transaction, including the storage capacities at the substations, power system connectivity to the external load, loading limits of the lines, etc. We discuss the amount of energy generated by the train and the profit percentage due to negotiation of this transaction with the external load. The profitability of the approach for the trains and the external load depend on the amount of energy requested, amount of regenerative energy available at the terminals, braking force, trip distance, maximum allowed speed, the difference between the DA and RT prices among other factors. The formulation of this transaction during a single trip is shown below.

$$\text{minimize} \quad \sum_{i=1}^{n} \lambda_i^{RT} \times (E'_{ACC_i} - E_{ACC_i}) + \lambda_i^{DA} \times E_{ACC_i}$$

subject to

$$E_{load}^{req} = E_{ACC_i}^{regen} \tag{4.2}$$

In addition to 4.2, the constraints 3.1 - 3.14 also have to be satisfied. Though this formulation is shown for a singletrip, this can be extended to any number of trips until the desired energy requested is achieved. The symbol E'_{ACC_i} denotes the excess energy consumed when participating in the transaction under pricing zone i, E_{ACC_i} denotes the contracted day-ahead energy consumption of ACC i with the ISO, λ_i^{RT} and λ_i^{DA} denote the electricity real-time and day-ahead price faced by the ACC i. The constraint 4.2 captures the energy transaction which means the the requested energy has to be satisfied by the train through regeneration. Symbols E_{load}^{req} and $E_{ACC_i}^{regen}$ represent the energy requested by the load and the energy regenerated by the train available at the ACC i.

For the results shown in Figures 27, we have taken the Acela trip from Boston to Providence, which is a 51.5 km, 20 min trip. For simulation purposes, we have assumed the DA and RT prices and explored the different conditions which enable profitability for both parties. There are 2 pricing zones ACC 1 and ACC 2 in where the DA price of zone 2 is 10% more than that of zone 1 whose DA price is taken to be 50 \$/MWh. Here in real-time, the prices of zone 1 increase and price of zone 2 decreases. Thus a load that is being priced under zone1 which requires emergency power faces very high electricity price.

Now, one train, if the load is small or multiple trains, if the load is big, can transact with this load, if it is profitable for both. We have varied the % change in RT prices and observed the results.

For the cases shown in Figure 27 and Table V, the RT price of zone 1 increases by 2 times than that of its DA price and RT price of zone 2 decreases by 50% than that of its DA price.This is a favorable condition for the train to transact with the external load requesting power in zone 1 because the train sees that the RT price of zone 2 has decreased and it can make up for the excess energy in the low-price zone 2.

Duration of Regenerative Braking (sec)	20	40	50	60
Energy Released (kWh)	33	69	86	103
Average electricity price for train before transaction ($/MWh)	51.17	51.17	51.17	51.17
Average Real-Time electricity price for load in Zone 1($/MWh)	100	100	100	100
Average electricity price for train for 0-100% profit ($/MWh)	54.11-48.02	57.02-44.62	58.64-43.16	63.1944.66

TABLE V: COMPARISON OF ENERGY TRANSACTION CASES WITH REGENERATIVE BRAKING

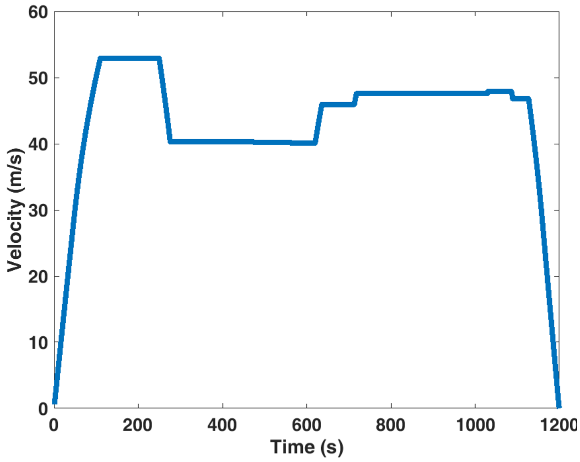

(a)

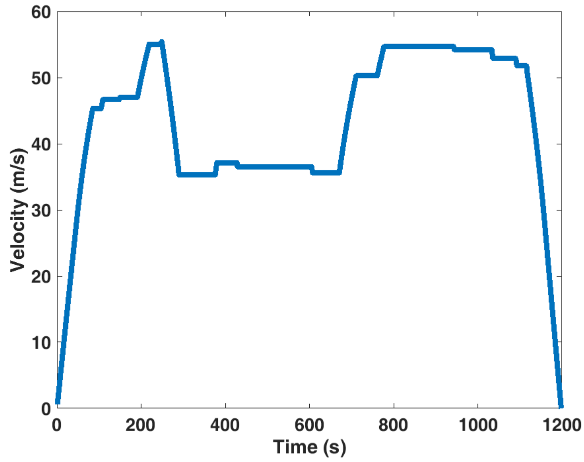

(b)

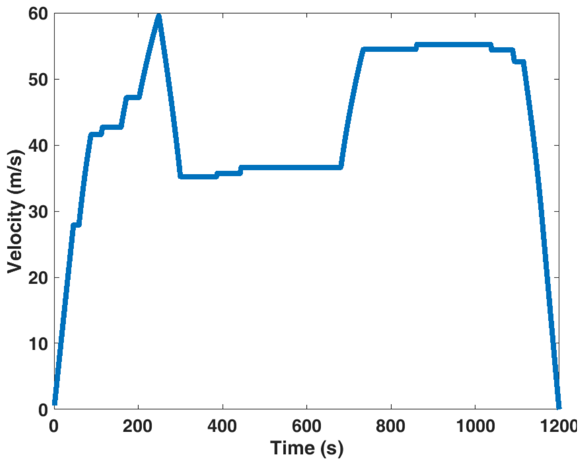

(c)

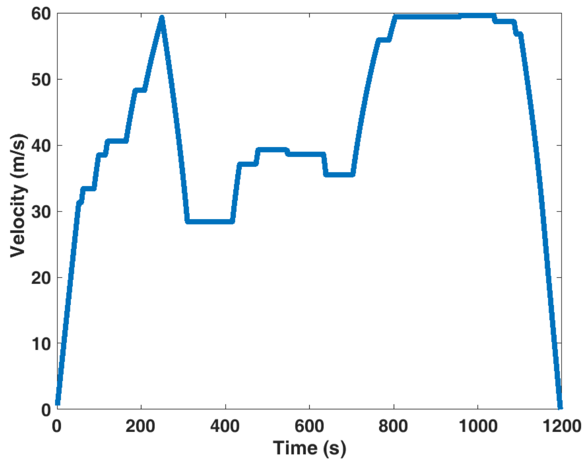

(d)

Figure 26: Velocity profiles during energy transaction with an external load (a) Energy transacted = 33kWh (b) Energy transacted=69 kWh (c) Energy transacted=86 kWh (d) Energy transacted=103 kWh

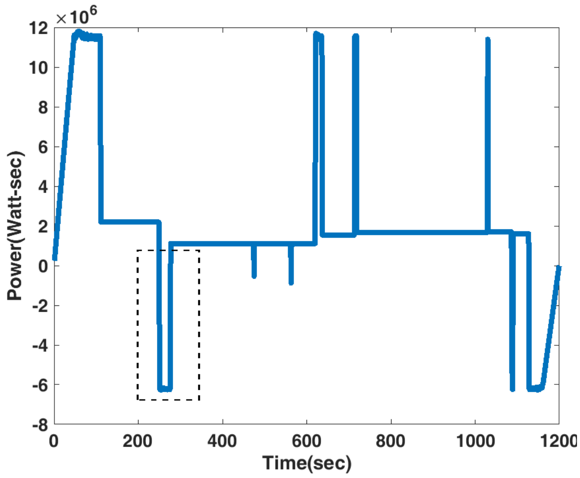

(a)

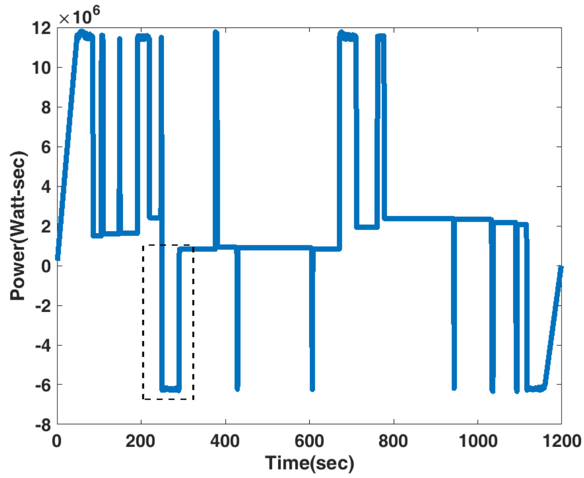

(b)

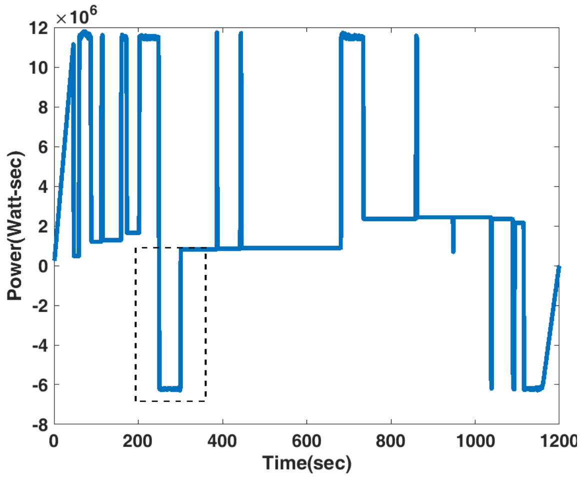

(c)

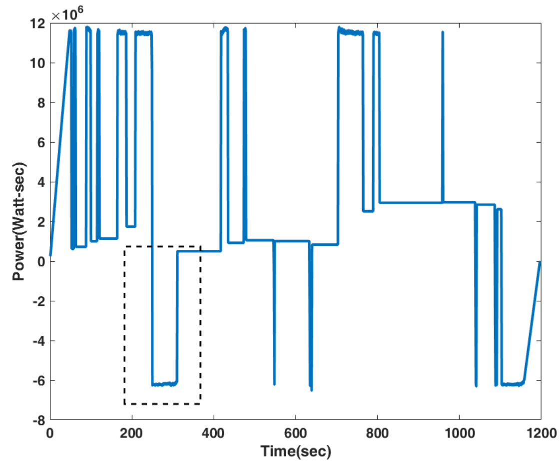

(d)

Figure 27: Power profiles during energy transaction with an external load (a) Energy transacted = 33kWh (b) Energy transacted=69 kWh (c) Energy transacted=86 kWh (d) Energy transacted=103 kWh

The power profile shows negative power during regeneration indicating that the energy is generated by the train. In the 20 sec column of Table V, the train brakes for 20 s to generate the requested amount of energy 33 kWh in zone 1. If it had not performed this transaction, the average electricity price felt by the train is shown in row 3, that is 51.17 \$/MWh. Since the RT electricity price is 100 \$/MWh in zone 1, the RT electricity price for the external load is shown by row 4. The last row indicates the dynamic real-time electricity price felt by the train upon transaction and negotiation. When the train sells this energy to the external load at 0 % profit, then it incurrs an additional cost of the trip, which increases the RT price felt by the train to 54.11 \$/MWh. When the train sells the energy to the load at same price as the ISO, the train receives 100 % profit reflected by 48 \$/MWh as the electicity price felt by it in this case. Successful negotiation between the train and the load lead to both parties sharing the profits. For example, charging the external load as 75 \$/MWh would reflect the dynamic RT price for the train as 49.5 \$/MWh, which is profitable for both parties. The maximum energy released by the train for this trip is around 100 kWh without violating the schedule.

Inorder to analyze the profitability of the approach, we changed different factors - like the factors by which RT price exceeds the DA price and efficiency of regenerative braking and analyzed the results. The cost reduction percentage is found by varying one factor while keeping the others constant. Maximum cost reduction is obtained by the train when it charges the external load at the same price as the market price. But the actual cost reduction or profit for the train is based on negotiation with the external load. For analysis purposes, we have found maximum cost reduction percentages and compared it in various cases. For the first plot in Figure 28a., we consider that the train sells the energy to the load at 90% of the actual real time price, which provides 10% profit to the load. We analyze the cost reduction

% for the train for various cases of RT prices- that is, when the RT prices are twice, thrice and 5 times that of DA price in zone 1. The plot clearly indicates that the profit for the train increases when the difference between RT and DA prices are higher. Larger amount of energy relinquished is comparatively less profitable when the difference between RT and DA prices are lesser.

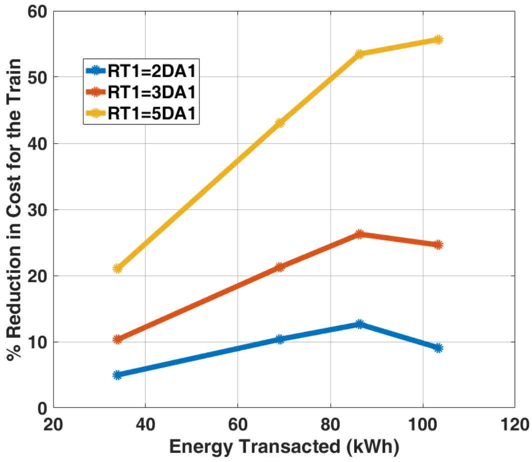

(a)

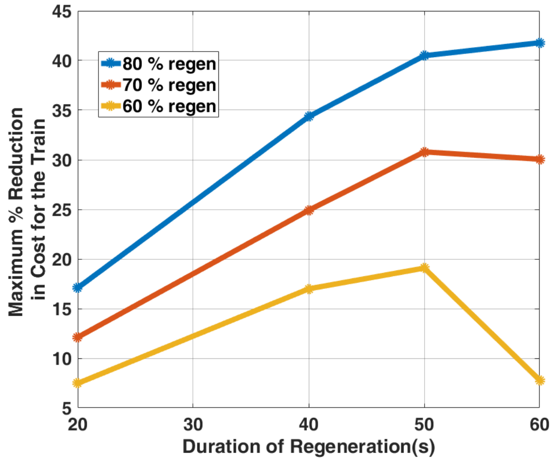

(b)

Figure 28: (a) Comparison of % reduction in cost of energy for the train after transaction with different RT prices (b) Comparison % reduction in cost of energy for the train after transaction with different regenerative braking efficiency percentages

The energy from regenerative braking depends on the braking force, which inturn is a function of the velocity of the train, among other factors. We have considered varying the efficiency factor with regenerative braking, which also implies the net energy available for the load shown in Figure 28. On performing regeneration for the same duration with different efficiency factors, the net energy available is different. We have compared the cases against the duration of regeneration for a case when the RT price is 3 times that of DA price in zone 1 and RT price is half of the DA price in zone 2. The profit certainly drops when the efficiency of regenerative braking is lesser and becomes not profitable when the efficiency of regeneration is 50% or lesser for larger amounts of energy transacted.

4.3 Transaction of Energy between Multiple Trains and External Load

For cases where the energy requirement is very large and a single train cannot relinquish that amount of energy without violating its schedule or when the ACC decides to distribute the load among 2 trains, then it leads to multiple trains transacting with a load as shown in Figure 29 The formulation can be modified as shown below:

$$\text{minimize} \quad \sum_{k=1}^{K}\sum_{i=1}^{n} \lambda_i^{RT} \times (E'_{ACC_i} - E_{ACC_i}) + \lambda_i^{DA} \times E_{ACC_i}$$

subject to

$$E_{ACC_i}^{req} = \sum_{k=1}^{K} E_{ACC_i}^{regen} \tag{4.3}$$

4.4 Transaction between Trains

Trains that apply regenerative braking when reaching a station can transfer this energy to an accelerating train that starts from the same station, enabled by the bidirectional power transfer system. This

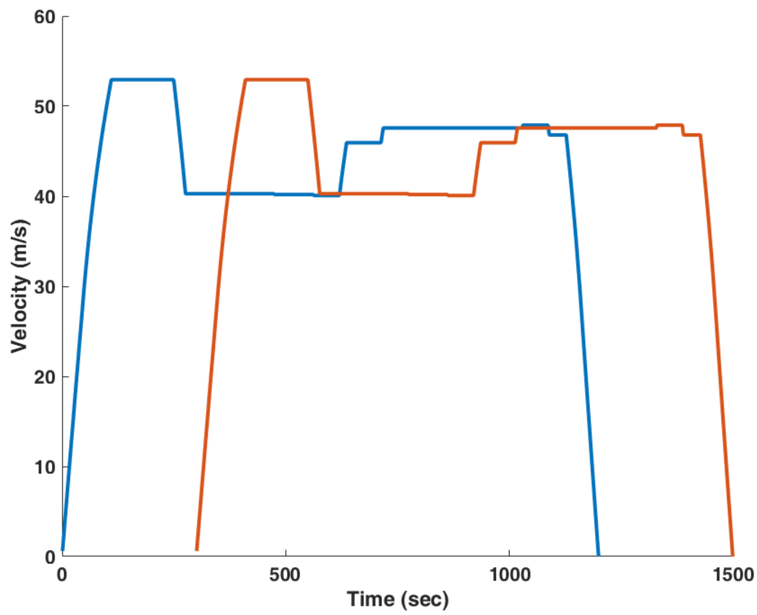

Figure 29: Two trains transacting with an external load

method of capturing the regenerative energy leads to lesser energy consumption on the whole and hence lesser energy cost (Sun et al., 2014). This multi-train coordination is utilized in timetable optimization and is not a driving strategy optimization. We analyze different cases of this regenerative energy tranfer between the trains leading to transaction between the trains.

- Transaction between trains where one train transacts with another train starting from a station.

  This can occur in the following scenarios :

  – In a situation where the price at which regenerative energy is sold back is lesser than the purchase cost of electricity, selling the energy back to the grid is less profitable than using the regenerative energy among the network of trains based on the day-ahead and real-time electricity prices the trains are subjected to. The ACCs communicate with each other and request for energy from other ACCs if the electriciy price in their region is lesser compared to itself.

– When there is an emergency situation in a particular substation and it limits the supplied power to the trains, regenerative energy from other trains crossing this station can be used to accelerate the starting trains.

ACC 1 requests energy from other ACCs due to one of the reasons mentioned above. The ACCs that are nearer to the ACC 1 and that have a lesser electricity price comparatively request the trains to accelerate so that when they cross the station that comes under ACC 1, they can transfer this energy to the accelerating trains. In the Figure 30 below, the blue curve is the velocity profile of the decelerating train, train 1. This train travels through ACC 1 and ACC 2.

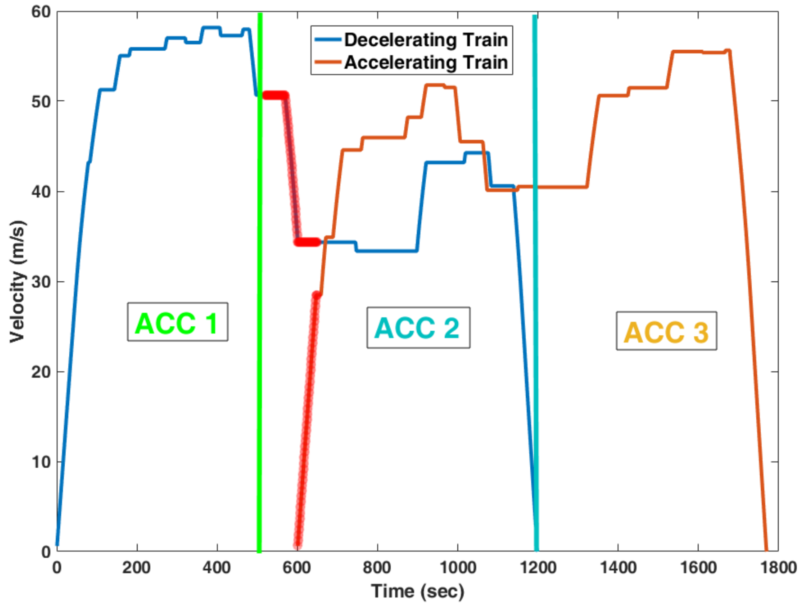

Figure 30: Transaction between trains where one train transacts with another train starting from a station

The substation under ACC 2 requests energy for accelerating train 2 and hence the train 1 decelerates when it enters the region of ACC 2 and transfers this regenerative energy to train 2. The highlighted portion indicates the energy transfer region. Electricity price in the region of ACC 1 is assumed to be 40 $/MWh, ACC 2 is 80 $/MWh and ACC 3 is 40 $/MWh. Assuming that the energy sold to the grid by the RSO is 2$ less than the price at which it is bought, this method of energy transaction leads to a savings of 15% as comapared to the case when the regenerated energy is sold back to the grid at a lower cost. Also when the substation under ACC 2 is stressed, this energy transaction would also help reduce the stress in the grid by interactively managing the regenerated energy within the train network.

- Transaction when one train has a latency during low price period.

  A train trip may have latencies due to various reasons like construction work in a track or weather conditions. When a latency happens in the region where the electricity price is low the train will have to travel at a slower speed when the electricity price is lower and will have to accelerate and travel at a higher speed with the electricity price is higher. This will lead to an increased cost of energy utilization for the trip. One such case is depicted in Figure 31.

The blue curve shows the profile of train 1 which has a latency due to an unexpected situation and cannot increase its speed beyond 30 m/s. Train 2 also has similar trip time as train 1 and starts its journey under ACC1. The train 2 had the original profile as shown in the dotted red curve. But the RSO determines that since this is a low price region and train 1 travels at a lower velocity during this period, it will have to compensate for the increased power consumption later on to catch up with its schedule. Thus it sends a command to ACC1 to allow for an increased power consumption by train 2 so that the total cost for the RSO does not increase. This shows an improvement of 3% for the 1200s trip and the price difference between the high and low price regions of the train is 20%.

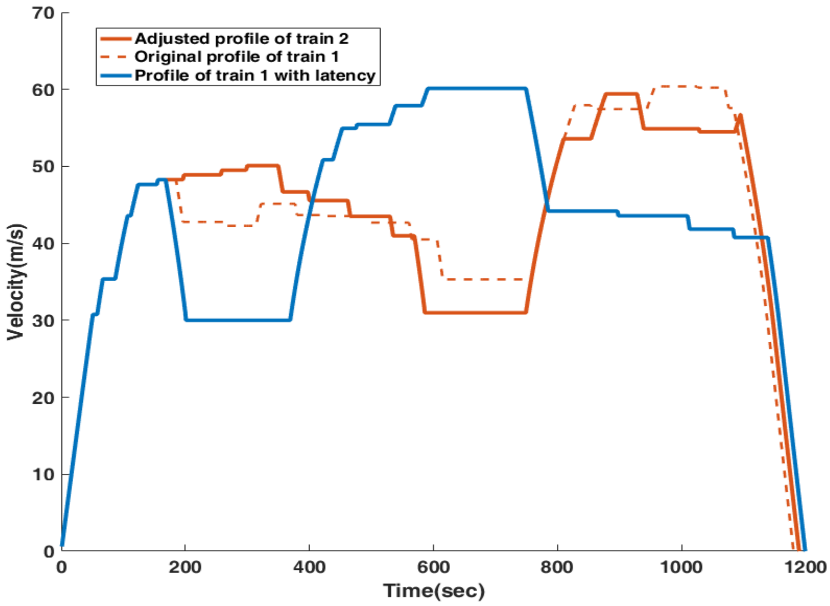

Figure 31: Transaction when one train has a latency during low price period

4.5 Summary

We have explored the concept of transaction between trains and external loads. This is a fairly novel concept and the participation of trains in the energy transaction can prove beneficial for both parties depending on the difference between the RT and DA prices. Though we have not analyzed the mechanism of how the transaction could take place, we analyzed different cases and developed parametric plots that show the cost reduction percentages under varios conditions of transaction. The results show profit for both the transacting parties.

CHAPTER 5

CONCLUSION AND SCOPE FOR FUTURE WORK

Our research on cost minimization strategies of electrical trains explored the methods of cost minimization optimization and energy transaction as the two strategies as key contributors towards cost reduction for the train operators. We have utilized the regenerative braking and analyzed its potential application to energy transaction. The physical constraints have been included while modeling and the time and space varying LMP prices have been considered to compare the results of cost optimization with the corresponding energy minimization cases for the high speed Acela route in the NEC. We also compared the results for planned high speed network in the US and explained the potential of employing this optimization method for obtaining the velocity profiles.

Ther other contribution of this thesis is in exploring the benefits of energy transaction for the railway operators. The trains are considered as flexible loads and this flexibility allows them to participate in energy transaction with external loads and with other trains. Using regenerative energy, the trains act as transactive nodes and respond to the request for energy by an external load and transfer this energy by behaving as generating sources. This transaction is settled based on the value negotiation between the parties concerned. We have also explored the situations where the trains can transact energy with other trains which would contribute to the total cost reduction of the train operator.

These results have been analyzed only for a fewer number of trains and they show promise in reducing the energy cost when extended to a large network of trains. One of the directions for future work would be extending the scalability of our approach for a large number of trains and exploring the transaction between different railway operators like Amtrak and MBTA in NEC, Metra, Amtrak and CTA in Chicago, etc. When the trans span larger distances (entire span of USA) and travel for longer duration, they pass through different pricing zones which could be under the jurisdiction of different ISOs and hence there lies a higher chance of reduction in energy cost when including these time and space varying LMP prices. Beyond these extensions mentioned so far, the flexibility of the trains can be used as a resource as expressed below:

- **As a Demand Response Resource** The RSO can be an active demand response resource. At times when the grid is stressed or congested heavily, the trains can alter their consumption to help achieve grid stabilization and various other benefits.
- **Participation in Energy Reserve Markets** Since the trains are flexible power consumers and generators, they can participate in energy reserve markets and can contribute to the reserve requirements of the grid.
- **Participation in Real-Time Market** The RSOs can participate in real time transactive market settlement by the ISO and can consume/generate to meet the demands. The different levels of transaction in a real-time market are shown in Figure 32(nsf,).
- **Coordination with energy storage devices and renewable generators** The RSOs can alter the power consumption of the trains such that they can charge the way-side energy storage devices via regeneration during low price and travel at higher speeds when more renewable generators are available and the electricity prices are negative.

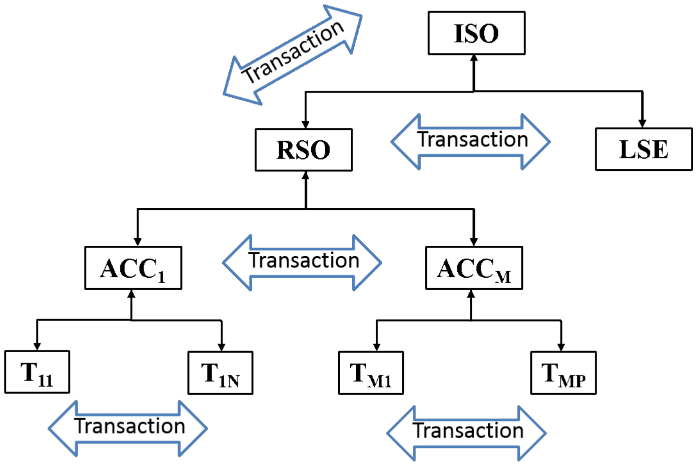

Figure 32: Real-time transaction opportunities for the RSO and ISO

There are three emerging energy-related areas of significant growth world-wide: electrical transportation, electrical-vehicle-based autonomous vehicles, and mega-microgrids (under the umbrella of smart grid) where our novel approaches may have direct utility thereby reducing cost of operation.

Appendices

Appendix A

SPANISH RAIL TRACK DATA

We have provided the Spanish track data that was used for the minimum time driving simulation. The speed limit sections, the gradient and the curvature resistance are shown here. The data for the simulation corresponds to the first 86.55 km of the high-speed line Madrid-Barcelona (Spain), starting at Madrid. There are two stations in this trip. First station at 64.4 km and the second station at 86.55 km from the start. The infrastructure of the high-speed trains roughly corresponds to high-speed trains Siemens Series 103.

Appendix A (Continued)

SLOPES	
Position (m)	Slope (expressed as sine of the angle)
0	0
1421	-0.01
2074.66	-0.009
2584.68	-0.009
3883.75	-0.001
4162.26	-0.012
4640.84	0.0117
5182.16	-0.006
5851.98	0.0091
6257.25	-0.013
7603.63	0.0017
8620.48	-0.006
8959.33	0.003
10317.49	0.02
11262.26	0.005
13479.1	0.025
15035.43	-0.018
16182.52	-0.005
17513.39	-0.01
18213.39	0.0153
20413.39	0.0087
21933.39	-0.025
25679.33	0.025
28410.45	-0.006
31837.11	-0.015
32995.33	0.025
34997.76	-0.003

(a)

SLOPES	
Position (m)	Slope (expressed as sine of the angle)
37500	0.005
38672	0.016
39719	0.002
40574	0.012
41727	0.01
46070	0.025
48848	0.017
49920	0.024
53114	0.005
54459	0.008
55780	0.005
59365	-0.005
62094	0.01
63060	0
66172	0.013
67260	0.004
69009	0.009
71125	0.006
72928	-0.009
73992	0.002
76483	-0.005
77569	0.003
79623	0.004
81014	-0.004
82343	0.009
84548	-0.005
85308	0.007

(b)

Gradient data of the track

Appendix A (Continued)

CURVES	
Position (m)	Radius (m) or 0 if straight
0	0
517.88	250
1085.79	0
1336.39	600
1401.32	0
1483.81	900
1693.21	1100
1894.27	900
2049.47	0
2695.57	700
3568.28	0
4063.01	-550
4188.35	0
4320.4	-600
4559.88	0
5247.68	2500
5582.81	-2500
6392.98	0
7326.35	-2500
7980.2	0
8227.98	2500
8751.43	0
9051.43	-2520
12998.1	0
16072.9	-4500
16741.2	0
17782.2	-4000

(a)

CURVES	
Position (m)	Radius (m) or 0 if straight
19781	0
20101	4000
24234	0
25391	-4500
26847	0
29630	7250
34131	0
34591	-7250
40307	0
40767	7250
42055	0
44746	10000
45793	0
47393	-7250
51877	0
52950	7250
54556	0
66323	-7250
68809	0
73118	-10000
73997	0
77344	10000
79352	0
80404	8000
83379	0

(b)

Radius of curvature of the track

Appendix A (Continued)

SPEED LIMITS	
Position (m)	Max. Speed (km/h)
0	350
517.88	72.3
1085.79	350
1336.39	112
1401.32	350
1483.81	137.2
1693.21	151.6
1894.27	137.2
2049.47	350
2695.57	121
3568.28	350
4063.01	107.2
4188.35	350
4320.4	112
4559.88	350
5247.68	228.6
5582.81	228.6
6392.98	350
7326.35	228.6
7980.2	350
8227.98	228.6
8751.43	350
9051.43	229.5
12998.1	350
16072.9	306.7
16741.2	350
17782.2	289.2

(a)

SPEED LIMITS	
Position (m)	Max. Speed (km/h)
0	350
517.88	72.3
1085.79	350
1336.39	112
1401.32	350
1483.81	137.2
1693.21	151.6
1894.27	137.2
2049.47	350
2695.57	121
3568.28	350
4063.01	107.2
4188.35	350
4320.4	112
4559.88	350
5247.68	228.6
5582.81	228.6
6392.98	350
7326.35	228.6
7980.2	350
8227.98	228.6
8751.43	350
9051.43	229.5
12998.1	350
16072.9	306.7
16741.2	350
17782.2	289.2

(b)

Speed limit data of the track

Appendix B

COPYRIGHT PERMISSIONS

In this appendix, we present the copyright permissions for the article, whose contents were used in this thesis.

IEEE COPYRIGHT AND CONSENT FORM

To ensure uniformity of treatment among all contributors, other forms may not be substituted for this form, nor may any wording of the form be changed. This form is intended for original material submitted to the IEEE and must accompany any such material in order to be published by the IEEE. Please read the form carefully and keep a copy for your files.

Cost-Reducing Optimization Strategies of Electrical Trains
Soumya Padmanabha Sarma, Sudip K. Mazumder, E. P. De La Fuente
2019 4th IEEE Workshop on the Electronic Grid (eGRID)

COPYRIGHT TRANSFER

The undersigned hereby assigns to The Institute of Electrical and Electronics Engineers, Incorporated (the "IEEE") all rights under copyright that may exist in and to: (a) the Work, including any revised or expanded derivative works submitted to the IEEE by the undersigned based on the Work; and (b) any associated written or multimedia components or other enhancements accompanying the Work.

GENERAL TERMS

1. The undersigned represents that he/she has the power and authority to make and execute this form.
2. The undersigned agrees to indemnify and hold harmless the IEEE from any damage or expense that may arise in the event of a breach of any of the warranties set forth above.
3. The undersigned agrees that publication with IEEE is subject to the policies and procedures of the IEEE PSPB Operations Manual.
4. In the event the above work is not accepted and published by the IEEE or is withdrawn by the author(s) before acceptance by the IEEE, the foregoing copyright transfer shall be null and void. In this case, IEEE will retain a copy of the manuscript for internal administrative/record-keeping purposes.
5. For jointly authored Works, all joint authors should sign, or one of the authors should sign as authorized agent for the others.
6. The author hereby warrants that the Work and Presentation (collectively, the "Materials") are original and that he/she is the author of the Materials. To the extent the Materials incorporate text passages, figures, data or other material from the works of others, the author has obtained any necessary permissions. Where necessary, the author has obtained all third party permissions and consents to grant the license above and has provided copies of such permissions and consents to IEEE

You have indicated that you DO wish to have video/audio recordings made of your conference presentation under terms and conditions set forth in "Consent and Release."

CONSENT AND RELEASE

1. In the event the author makes a presentation based upon the Work at a conference hosted or sponsored in whole or in part by the IEEE, the author, in consideration for his/her participation in the conference, hereby grants the IEEE the unlimited, worldwide, irrevocable permission to use, distribute, publish, license, exhibit, record, digitize, broadcast, reproduce and archive, in any format or medium, whether now known or hereafter developed: (a) his/her presentation and comments at the conference; (b) any written materials or multimedia files used in connection with his/her presentation; and (c) any recorded interviews of him/her (collectively, the "Presentation"). The permission granted includes the transcription and reproduction of the Presentation for inclusion in products sold or distributed by IEEE and live or recorded broadcast of the Presentation during or after the conference.
2. In connection with the permission granted in Section 1, the author hereby grants IEEE the unlimited, worldwide, irrevocable right to use his/her name, picture, likeness, voice and biographical information as part of the advertisement, distribution and sale of products incorporating the Work or Presentation, and releases IEEE from any claim based on right of privacy or publicity.

BY TYPING IN YOUR FULL NAME BELOW AND CLICKING THE SUBMIT BUTTON, YOU CERTIFY THAT SUCH ACTION CONSTITUTES YOUR ELECTRONIC SIGNATURE TO THIS FORM IN ACCORDANCE WITH UNITED STATES LAW, WHICH AUTHORIZES ELECTRONIC SIGNATURE BY AUTHENTICATED REQUEST FROM A USER OVER THE INTERNET AS A VALID SUBSTITUTE FOR A WRITTEN SIGNATURE.

SOUMYA PADMANABHA SARMA	07-01-2020
Signature	**Date (dd-mm-yyyy)**

Information for Authors

AUTHOR RESPONSIBILITIES

The IEEE distributes its technical publications throughout the world and wants to ensure that the material submitted to its publications is properly available to the readership of those publications. Authors must ensure that their Work meets the requirements as stated in section 8.2.1 of the IEEE PSPB Operations Manual, including provisions covering originality, authorship, author responsibilities and author misconduct. More information on IEEE's publishing policies may be found at http://www.ieee.org/publications_standards/publications/rights/authorrightsresponsibilities.html Authors are advised especially of IEEE PSPB Operations Manual section 8.2.1.B12: "It is the responsibility of the authors, not the IEEE, to determine whether disclosure of their material requires the prior consent of other parties and, if so, to obtain it." Authors are also advised of IEEE PSPB Operations Manual section 8.1.1B: "Statements and opinions given in work published by the IEEE are the expression of the authors."

RETAINED RIGHTS/TERMS AND CONDITIONS

- Authors/employers retain all proprietary rights in any process, procedure, or article of manufacture described in the Work.
- Authors/employers may reproduce or authorize others to reproduce the Work, material extracted verbatim from the Work, or derivative works for the author's personal use or for company use, provided that the source and the IEEE copyright notice are indicated, the copies are not used in any way that implies IEEE endorsement of a product or service of any employer, and the copies themselves are not offered for sale.
- Although authors are permitted to re-use all or portions of the Work in other works, this does not include granting third-party requests for reprinting, republishing, or other types of re-use.The IEEE Intellectual Property Rights office must handle all such third-party requests.
- Authors whose work was performed under a grant from a government funding agency are free to fulfill any deposit mandates from that funding agency.

AUTHOR ONLINE USE

- **Personal Servers**. Authors and/or their employers shall have the right to post the accepted version of IEEE-copyrighted articles on their own personal servers or the servers of their institutions or employers without permission from IEEE, provided that the posted version includes a prominently displayed IEEE copyright notice and, when published, a full citation to the original IEEE publication, including a link to the article abstract in IEEE Xplore. Authors shall not post the final, published versions of their papers.
- **Classroom or Internal Training Use.** An author is expressly permitted to post any portion of the accepted version of his/her own IEEE-copyrighted articles on the author's personal web site or the servers of the author's institution or company in connection with the author's teaching, training, or work responsibilities, provided that the appropriate copyright, credit, and reuse notices appear prominently with the posted material. Examples of permitted uses are lecture materials, course packs, e-reserves, conference presentations, or in-house training courses.
- **Electronic Preprints.** Before submitting an article to an IEEE publication, authors frequently post their manuscripts to their own web site, their employer's site, or to another server that invites constructive comment from colleagues. Upon submission of an article to IEEE, an author is required to transfer copyright in the article to IEEE, and the author must update any previously posted version of the article with a prominently displayed IEEE copyright notice. Upon publication of an article by the IEEE, the author must replace any previously posted electronic versions of the article with either (1) the full citation to the

CITED LITERATURE

[ig,] LMP. http://iso-ne.com.

[dem,] Maximum demand charge rates for commercial and industrial electricity tariffs in the United States. National Renewable Energy Laboratory. https://dx.doi.org/10.7799/1392982.

[nsf,] NSF Award. http://https://www.nsf.gov/awardsearch/showAward?AWD_ID=1644874&HistoricalAwards=false.

[ush,] U.s. high speed railways. http://ushsr.com.

[Açıkbaş and Söylemez, 2008] Açıkbaş, S. and Söylemez, M.: Coasting point optimisation for mass rail transit lines using artificial neural networks and genetic algorithms. IET Electric Power Applications, 2(3):172–182, 2008.

[Behboodi et al. , 2018] Behboodi, S., Chassin, D. P., Djilali, N., and Crawford, C.: Transactive control of fast-acting demand response based on thermostatic loads in real-time retail electricity markets. Applied Energy, 210:1310–1320, 2018.

[Benjamin et al. , 1989] Benjamin, B., Milroy, I., Pudney, P., et al.: Energy-efficient operation of long-haul trains. In Fourth International Heavy Haul Railway Conference 1989: Railways in Action; Preprints of Papers, The, page 369. Institution of Engineers, Australia, 1989.

[Bocharnikov et al. , 2010] Bocharnikov, Y., Tobias, A., and Roberts, C.: Reduction of train and net energy consumption using genetic algorithms for trajectory optimisation. 2010.

[Cai et al. , 2017] Cai, B.-G., Sheng, Z., ShangGuan, W., and Sun, J.: Train trajectory optimization with dynamic headway. In 2017 36th Chinese Control Conference (CCC), pages 9920–9925. IEEE, 2017.

[Calderaro et al. , 2015] Calderaro, V., Galdi, V., Graber, G., and Piccolo, A.: Deterministic vs heuristic algorithms for eco-driving application in metro network. In 2015 International Conference on Electrical Systems for Aircraft, Railway, Ship Propulsion and Road Vehicles (ESARS), pages 1–6. IEEE, 2015.

[Chang and Sim, 1997] Chang, C. and Sim, S.: Optimising train movements through coast control using genetic algorithms. IEE Proceedings-Electric Power Applications, 144(1):65–73, 1997.

[Chen et al. , 2015] Chen, E., Bu, B., and Wenzhe, S.: An energy-efficient operation approach based on the utilization of regenerative braking energy among trains. In Intelligent Transportation Systems (ITSC), 2015 IEEE 18th International Conference on, pages 2606–2611. IEEE, 2015.

[Cheng et al. , 2000] Cheng, J., Cheng, J., Song, J., and Zhao, P.: Algorithms on optimal driving strategies for train control problem. In Proceedings of the 3rd World Congress on Intelligent Control and Automation (Cat. No. 00EX393), volume 5, pages 3523–3527. IEEE, 2000.

[Chevrier et al. , 2011] Chevrier, R., Marlière, G., Vulturescu, B., and Rodriguez, J.: Multi-objective evolutionary algorithm for speed tuning optimization with energy saving in railway: Application and case study. In RailRome 2011, 2011.

[De La Fuente et al. , 2014] De La Fuente, E. P., Mazumder, S. K., and Franco, I. G.: Railway electrical smart grids: An introduction to next-generation railway power systems and their operation. IEEE Electrification Magazine, 2(3):49–55, 2014.

[Domínguez et al. , 2014] Domínguez, M., Fernández-Cardador, A., Cucala, A. P., Gonsalves, T., and Fernández, A.: Multi objective particle swarm optimization algorithm for the design of efficient ato speed profiles in metro lines. Engineering Applications of Artificial Intelligence, 29:43–53, 2014.

[Dong et al. , 2014] Dong, H.-Y., Liu, Y., and Yang, L.-X.: Study on multi-objective optimization of high-speed train operation based on clonal selection algorithm. In Proceeding of the 11th World Congress on Intelligent Control and Automation, pages 1755–1760. IEEE, 2014.

[Fleck et al. , 2016] Fleck, M., Khayyam, S., and Monti, A.: Day-ahead optimization for railway energy management system. In 2016 International Conference on Electrical Systems for Aircraft, Railway, Ship Propulsion and Road Vehicles & International Transportation Electrification Conference (ESARS-ITEC), pages 1–8. IEEE, 2016.

[Franke et al. , 2000] Franke, R., Terwiesch, P., and Meyer, M.: An algorithm for the optimal control of the driving of trains. In Proceedings of the 39th IEEE Conference on Decision and Control (Cat. No. 00CH37187), volume 3, pages 2123–2128. IEEE, 2000.

[GabrielRéchard, 2017] GabrielRéchard, R.: Recovering energy from train braking for traction and grid use. Energy Procedia ELSEVIER, 2017.

[Gordon and Jaboolian, 1932] Gordon, W. and Jaboolian, E.: A review of european railway electrification. Electrical Engineering, 51(4):244–252, 1932.

[Hammerstrom et al. , 2009] Hammerstrom, D., Oliver, T., Melton, R., and Ambrosio, R.: Standardization of a hierarchical transactive control system. Grid Interop, 9:35–42, 2009.

[Hao et al. , 2016] Hao, H., Corbin, C. D., Kalsi, K., and Pratt, R. G.: Transactive control of commercial buildings for demand response. IEEE Transactions on Power Systems, 32(1):774–783, 2016.

[He et al. , 2019] He, D., Lu, G., and Yang, Y.: Research on optimization of train energy-saving based on improved chicken swarm optimization. IEEE Access, 7:121675–121684, 2019.

[Howlett et al. , 1994] Howlett, P., Milroy, I., and Pudney, P.: Energy-efficient train control. Control Engineering Practice, 2(2):193–200, 1994.

[Howlett, 1990] Howlett, P.: An optimal strategy for the control of a train. The ANZIAM Journal, 31(4):454–471, 1990.

[Howlett, 1996] Howlett, P.: Optimal strategies for the control of a train. Automatica, 32(4):519–532, 1996.

[Hu et al. , 2014] Hu, W., Sun, Q., and Lv, J.: Research on subway trains' energy conservation running based on pso. In 2014 International Conference on Information Science, Electronics and Electrical Engineering, volume 2, pages 1325–1329. IEEE, 2014.

[Huang et al. , 2010] Huang, P., Kalagnanam, J., Natarajan, R., Hammerstrom, D., Melton, R., Sharma, M., and Ambrosio, R.: Analytics and transactive control design for the pacific northwest smart grid demonstration project. In 2010 First IEEE International Conference on Smart Grid Communications, pages 449–454. IEEE, 2010.

[Ichikawa, 1968] Ichikawa, K.: Application of optimization theory for bounded state variable problems to the operation of train. Bulletin of JSME, 11(47):857–865, 1968.

[Jha et al. , 2007] Jha, M. K., Schonfeld, P., and Samanta, S.: Optimizing rail transit routes with genetic algorithms and geographic information system. Journal of Urban Planning and Development, 133(3):161–171, 2007.

[Jiaxin and Howlett, 1993] Jiaxin, C. and Howlett, P.: A note on the calculation of optimal strategies for the minimization of fuel consumption in the control of trains. IEEE Transactions on Automatic Control, 38(11):1730–1734, 1993.

[Katipamula et al. , 2006] Katipamula, S., Chassin, D. P., Hatley, D. D., Pratt, R. G., and Hammerstrom, D. J.: Transactive controls: A market-based gridwisetm controls for building systems. Technical report, Pacific Northwest National Lab.(PNNL), Richland, WA (United States), 2006.

[Keskin and Karamancioglu, 2016] Keskin, K. and Karamancioglu, A.: Application of firefly algorithm to train operation. In 2016 IEEE 8th International Conference on Intelligent Systems (IS), pages 692–697. IEEE, 2016.

[Khmelnitsky, 2000] Khmelnitsky, E.: On an optimal control problem of train operation. IEEE transactions on automatic control, 45(7):1257–1266, 2000.

[Kim et al. , 2013] Kim, Y.-G., Jeon, C.-S., Kim, S.-W., and Park, T.-W.: Operating speed pattern optimization of railway vehicles with differential evolution algorithm. International Journal of Automotive Technology, 14(6):903–911, 2013.

[Kroon and Peeters, 2003] Kroon, L. G. and Peeters, L. W.: A variable trip time model for cyclic railway timetabling. Transportation Science, 37(2):198–212, 2003.

[Lee et al. , 1982] Lee, D., Milroy, I. P., Tyler, K., et al.: Application of pontryagin's maximum principle to the semi-automatic control of rail vehicles. In Second Conference on Control Engineering 1982: Merging of Technology and Theory to Solve Industrial Automation Problems; Preprints of Papers, page 233. Institution of Engineers, Australia, 1982.

[Li et al. , 2011] Li, L., Dong, W., Ji, Y., and Zhang, Z.: An optimal driving strategy for high-speed electric train. In Proceedings of the 30th Chinese Control Conference, pages 5899–5904. IEEE, 2011.

[Lin and Sheu, 2011] Lin, W.-S. and Sheu, J.-W.: Optimization of train regulation and energy usage of metro lines using an adaptive-optimal-control algorithm. IEEE Transactions on Automation Science and Engineering, 8(4):855–864, 2011.

[Liu et al. , 2017] Liu, Z., Wu, Q., Huang, S., and Zhao, H.: Transactive energy: A review of state of the art and implementation. In 2017 IEEE Manchester PowerTech, pages 1–6. IEEE, 2017.

[Liu et al. , 2018] Liu, Z., Wu, Q., Ma, K., Shahidehpour, M., Xue, Y., and Huang, S.: Two-stage optimal scheduling of electric vehicle charging based on transactive control. IEEE Transactions on Smart Grid, 2018.

[Lu et al. , 2013] Lu, S., Hillmansen, S., Ho, T. K., and Roberts, C.: Single-train trajectory optimization. IEEE Transactions on Intelligent Transportation Systems, 14(2):743–750, 2013.

[Lu et al. , 2016] Lu, S., Wang, M. Q., Weston, P., Chen, S., and Yang, J.: Partial train speed trajectory optimization using mixed-integer linear programming. IEEE Transactions on Intelligent Transportation Systems, 17(10):2911–2920, 2016.

[Martínez Fernández et al. , 2019] Martínez Fernández, P., S Zuriaga, P., Villalba Sanchís, I., and I Franco, R.: Neural networks for modelling the energy consumption of metro trains. Proceedings of the Institution of Mechanical Engineers, Part F: Journal of Rail and Rapid Transit, page 0954409719861595, 2019.

[Melton, 2015] Melton, R.: Gridwise transactive energy framework version 1. Grid-714 Wise Archit. Council, Richland, WA, USA, Tech. Rep. PNNL-22946, 715:716, 2015.

[Milroy, 1980] Milroy, I. P.: Aspects of automatic train control. Doctoral dissertation, © Ian Peter Milroy, 1980.

[Miyatake and Ko, 2010] Miyatake, M. and Ko, H.: Optimization of train speed profile for minimum energy consumption. IEEJ Transactions on Electrical and Electronic Engineering, 5(3):263–269, 2010.

[Moyer, 2016] Moyer, B.: Solutonary Rail: A People-Powered Campaign to Electrify America's Railroads and Open Corridors to a Clean Energy Future. Backbone Campaign, 2016.

[Nachtigall and Voget, 1997] Nachtigall, K. and Voget, S.: Minimizing waiting times in integrated fixed interval timetables by upgrading railway tracks. European journal of operational research, 103(3):610–627, 1997.

[Nasri et al. , 2010] Nasri, A., Moghadam, M. F., and Mokhtari, H.: Timetable optimization for maximum usage of regenerative energy of braking in electrical railway systems. In SPEEDAM 2010, pages 1218–1221. IEEE, 2010.

[Novak et al. , 2017] Novak, H., Lešić, V., and Vašak, M.: Hierarchical coordination of trains and traction substation storages for energy cost optimization. In 2017 IEEE 20th International Conference on Intelligent Transportation Systems (ITSC), pages 1–6. IEEE, 2017.

[Novak et al. , 2018] Novak, H., Lešić, V., and Vašak, M.: Hierarchical model predictive control for coordinated electric railway traction system energy management. IEEE Transactions on Intelligent Transportation Systems, 2018.

[Peeters, 2003] Peeters, L.: Cyclic railway timetable optimization. Number EPS-2003-022-LIS. 2003.

[Pineda-Jaramillo et al. , 2018] Pineda-Jaramillo, J. D., Insa, R., and Martínez, P.: Modeling the energy consumption of trains by applying neural networks. Proceedings of the Institution of Mechanical Engineers, Part F: Journal of Rail and Rapid Transit, 232(3):816–823, 2018.

[Sheu and Lin, 2012] Sheu, J.-W. and Lin, W.-S.: Energy-saving automatic train regulation using dual heuristic programming. IEEE Transactions on vehicular Technology, 61(4):1503–1514, 2012.

[Sicre et al. , 2014] Sicre, C., Cucala, A., and Fernández-Cardador, A.: Real time regulation of efficient driving of high speed trains based on a genetic algorithm and a fuzzy model of manual driving. Engineering Applications of Artificial Intelligence, 29:79–92, 2014.

[Sijie and Chen-Ching, 2017] Sijie, C. and Chen-Ching, L.: From demand response to transactive energy: state of the art. Journal of Modern Power Systems and Clean Energy, 5(1):10–19, 2017.

[Somasundaram et al. , 2014] Somasundaram, S., Pratt, R., Akyol, B., Fernandez, N., Foster, N., Katipamula, S., Mayhorn, E., Somani, A., Steckley, A., and Taylor, Z.: Reference guide for a transaction-based building controls framework. Pacific Northwest National Laboratory, 2014.

[Soumya P. Sarma, 2019] Soumya P. Sarma, S. K. M.: Cost optimization strategies of electrical trains. In IEEE eGrid 2019. IEEE, 2019.

[Storn and Price, 1997] Storn, R. and Price, K.: Differential evolution–a simple and efficient heuristic for global optimization over continuous spaces. Journal of global optimization, 11(4):341–359, 1997.

[Subbarao et al. , 2013] Subbarao, K., Fuller, J. C., Kalsi, K., Somani, A., Pratt, R. G., Widergren, S. E., and Chassin, D. P.: Transactive control and coordination of distributed assets for ancillary services. Technical report, Pacific Northwest National Lab.(PNNL), Richland, WA (United States), 2013.

[Sun et al. , 2014] Sun, X., Cai, H., Hou, X., Zhang, M., and Dong, H.: Regenerative braking energy utilization by multi train cooperation. In Intelligent Transportation Systems (ITSC), 2014 IEEE 17th International Conference on, pages 139–144. IEEE, 2014.

[Van Lessen, 1950] Van Lessen, H.: Electric and diesel-electric traction on the netherlands railways. Proceedings of the IEE-Part I: General, 97(104):63–76, 1950.

[Widergren et al. , 2014] Widergren, S., Fuller, J., Marinovici, C., and Somani, A.: Residential transactive control demonstration. In ISGT 2014, pages 1–5. IEEE, 2014.

[Xu et al. , 2014] Xu, Y., Zhao, X., Wang, L., Liu, X., and Zhang, Q.: Optimal control of automatic train operation based on multi-scale dynamic programming. In Proceedings of the 33rd Chinese Control Conference, pages 3429–3433. IEEE, 2014.

[Yao and Zhang, 2017] Yao, Y. and Zhang, P.: Transactive control of air conditioning loads for mitigating microgrid tie-line power fluctuations. In 2017 IEEE Power & Energy Society General Meeting, pages 1–5. IEEE, 2017.

[Zhu et al. , 2018] Zhu, A., Ma, X., Duan, Y., Li, J., and Li, J.: Operation optimization of train based on firefly algorithm. In 2018 IEEE 4th Information Technology and Mechatronics Engineering Conference (ITOEC), pages 1624–1628. IEEE, 2018.

VITA

SOUMYA PADMANABHA SARMA

Education	M.S. Electrical and Computer Engineering University of Illinois at Chicago	2018 – 2020
	M.S. Electrical Engineering Indian Institute of Technology Madras, India	2014 – 2017
	B.Tech. Electrical and Electronics Engineering College of Engineering Trivandrum, India	2009 – 2013
Accepted Publication	**Soumya P.**, Sudip K. Mazumder and Eduardo Pilo "Cost Reducing Optimization Strategies in Electrical Trains ", (*IEEE eGrid, China*) IEEE, 2019.	
Publications	**Soumya P.** and K.S. Swarup, "Optimal Capacitor Placement in Smart Grid using Demand Side Management as a Resource ", (*IEEE Power and Energy Conference at Illinois (PECI),*) IEEE, 2017.	
	Soumya P. and K.S. Swarup, "Reliability Improvements Considering Reactive Power Aspects in a Smart Grid with Demand Side Management", (*IEEE National Power System Conference, India,*) IEEE, 2016.	
	Pranjal Verma, **Soumya P.** and K.S. Swarup, "Optimal Day-Ahead Scheduling in Smart Grid with Demand Side Management", (*IEEE International Conference on Power Systems, India,*) IEEE, 2016.	
Awards	Best project award in the area of Genetic Algorithms and Evolutionary Computation, Indian Institute of Technology Madras.	
	Silver medalist in the Department of Electrical Engineering, College of Engineering Trivandrum, India.	
Experience	Research Assistant at LESES, UIC. Teaching Assistant at ECE Dept., UIC	